Escola Tècnica Superior d'Enginyeria

Electrònica i Informàtica La Salle

Treball Final de Màster

Màster Universitari en Enginyeria de Telecomunicació

Antenna Booster Antenna Technology for Smartwatches

Alumne

Ignasi Anglada Florensa

Professor Ponent

Dra. Aurora Andújar / Dr. Jaume Anguera

ACTA DE L'EXAMEN

DEL TREBALL DE FINAL DE MASTER

Reunit el Tribunal qualificador en el dia de la data, l'alumne

D. Ignasi Anglada Florensa

va exposar el seu Treball de Final de Màster, el qual va tractar sobre el tema següent: Antenna Booster Antenna Technology for Smartwatches

Acabada l'exposició i contestades per part de l'alumne les objeccions formulades pels Srs. membres del tribunal, aquest valorà l'esmentat Treball amb la qualificació de

Barcelona,

VOCAL DEL TRIBUNAL VOCAL DEL TRIBUNAL

PRESIDENT DEL TRIBUNAL

Abstract

As long as new technologies appear, the need for smaller and more customizable antennas has become a reality. When the first smartwatches came out, they were only able to work if connected to a smartphone through Bluetooth. Therefore, the next step in the design of this devices is making them able to be autonomous.

This study focuses on designing a small enough antenna system to fit in a wearable device (i.e. a smartwatch) which is also capable of working with LTE bands. To do so, the proposed antenna will be a radiating system composed by a Antenna booster and a radiating surface as small as possible.

Multiple candidates have been designed and studied, and their properties have been measured in order to find out how good they fix the described problem.

This project, as long as the research done, has been supervised by PhD. Jaume Anguera and PhD. Aurora Andújar.

Acknowledgement

I would like to thank Fractus Antennas for letting me develop this project within their headquarters in Sant Cugat, Barcelona, and for letting me use their materials and resources. Without that, this project would never have been possible.

Also, thanks to my friend Lluis for introducing me this world and making the first contact between me and Fractus Antennas.

And finally, I would like to express my infinite gratitude to Jaume and Aurora, not only for their technical teachings but also for their patience and support. It has been a real pleasure and an honour to work by their side.

Index

Acronyms

PDA: Personal Digital Assistant.

GPB: Antenna booster.

MWO: Microwave Office.

IFA: Inverted-F Antenna.

ABS: Acrylonitrile Butadiene Styrene.

HF: High Frequency

SWR: Standing Wave Ratio

1 Introduction

1.1 The evolution of telecommunication

1.1.1 The origin of civilizations

It is widely accepted that the origins of telecommunications go back to Africa, America and Asia with the smoke and sound signals that tribes used to send short and predefined messages between their members. As time passed, those tribes discovered that the safer way to prosper was to stay together, leading to the formation of the first societies, and being able to warn their members for dangers has been a clue fact.

Thousands of years later, and in the middle of the information society era, it can be assured that communication between individuals has played a vital role on the evolution from those first societies to the current times. It has been thanks to the communication that societies started growing, leading to the formation of major civilizations which continued using communication for learning and sharing their knowledge.

Today, the growth of communications has not only become exponential but the main purpose of some of the biggest enterprises in the world. So is this that three out of the fifteen largest companies in the world are engaged in the research and commercialization of telecommunication technologies and devices [1] .

1.1.2 The materialization of telecommunications

Before electricity was discovered, humans have always used all the existing resources to improve their telecommunication possibilities, like in the ancient Greece, where fire signals were used to send simple and predefined messages through long distances.

It wasn't until 1871 that Antonio Meucci first tried to patent the first model of a telephone from which there is a register. As he couldn't afford the cost of that patent, 5 years later a new patent was conceded to Alexander Graham Bell, who was considered as the inventor of that device until 2002. In that year, the US Congress officially concluded that Meucci's achievements had to be credited and so recognized the Italian as the true inventor of the telephone [2] .

From the moment the first phone was created, this device has experimented several improves on an exponential evolution, ending in today's smartphones. It is, so, easy to imagine that, from the moment telephones saw the light, a huge industry appeared around them.

In 1994, IBM released Simon Personal Communicator, considered the first smartphone ever [3] , which had the capability of receiving faxes and mails. This device (Figure 1) was the first to combine a PDA and a mobile phone. The main problems were its battery, which lasted only for 1 hour, and its size, much bigger than mobile phones where in those times.

From the release of this device on, several companies started to release their own smartphones, which every year showed bigger screens, better resolution and faster connections. Those companies also started creating new complements to interact with every new smartphone, what leaded to the main character of this project.

Figure 1: Simon Personal Communicator

This way, in 2007 Sony Ericsson launched the MBW-150, the first smartwatch to connect with a mobile phone using Bluetooth [4] . It had several limitations, as a very short battery-life and compatibility problems with non-Sony Ericsson phones, but it settled a whole new world of opportunities to both technology and jewellery companies.

This new world saw its greatest revolution in 2014, when LG and Samsung launched the first smartwatches that not only connected with their smartphones but also had de capability of handling own applications. Some months later, on April 2015, Apple also entered this competition with the launch of their first Apple Watch, which tried to compete at the same time against smartwatches and classic luxury watches (Figure 2).

Figure 2: First Apple Watch

Anyway, those wearables had still a lot to improve. In the following years, they started to become water resistant, to incorporate longer lasting batteries and, most important, to being more independent. This last point meant that those wearables needed to allow mobile phone technology, to move from being a smartwatch complement to a new device capable of substituting people's mobile phones.

That improvement came also in 2014, when many companies started to sell smartwatches capable of handling mobile telecommunications. Now, the aim for that companies is to apply the same technology that actual smartphones use in terms of signal quality and capacity, and this is also this project's main goal.

1.2 Purpose of the project

Trying to be part of smartwatches' evolution, this project focuses on building a smartwatch antenna system based on antenna booster compatible with LTE technology.

To reach the main goal, several steps must be followed, so it can be said that there are first sub-objectives to accomplish in order to reach the main purpose. Those initial steps can be summarized as follows:

- To understand today's antennas limitations and identify how to improve the situation.
- Learning how to work in a development environment such as Fractus Antennas' headquarters. This also implies getting to manipulate both specific antennas design and simulation programs and physical devices to implement and measure the designed antennas properties.
- Reading the state of the art to situate in the actuality in what refers to smartwatches' antennas.
- To be able to analyse the obtained results and determine whether they are good or not.
- To analyse the market and decide if the final result is good enough to fit in actual smartwatches manufacturing.

1.3 Document organization

In order to achieve the different defined goals, this project has been split in different stages. To allow the reader seeing it this way, this document has been structured in several chapters that try to represent each stage.

This first chapter introduces how communications evolved and what are the actual technologies and their limitations, leading this to define a clear objective in the design of a new antenna.

In the second chapter, several scientific paper will be summarized, and conclusions will be outlined in order to choose the right way of focusing the efforts for this project.

Along the third chapter, the design and simulation of several prototypes will be carried out. Once simulated, each prototype properties and particular results will tell if they are viable for moving to the next stage and so become a candidate.

At the fourth chapter, candidates will be physically implemented and putted under study. By doing so, previous chapter predictions will be certified or refused. This particular objective of this stage is to leave a solid candidate to consider as viable for its integration with actual devices.

Finally, the fifth chapter will consider all of the previous results to conclude if the main objectives have been achieved and if a solid solution has been found.

2 State-of-the-art

2.1 Introduction

In this section, multiple scientific papers are studied in order to understand the current state of smartwatch antennas technology and where are they leading to.

Along the different reviewed papers and articles, different smartwatch antennas models are discussed, including those that enable GPS, Bluetooth or MIMO.

2.2 Review of prior art

2.2.1 Metal-Frame GPS Antenna for Smartwatch Applications

The main goal of the investigation this article [5] talks about is to implement an antenna that allows smartwatches to have GPS signal independently from a smartphone. The proposed model is a loop antenna placed at the bottom of the top metal frame of the watch, with a size of 7mm x 35mm x 40mm (Figure 3).

The first parameter considered has been the position of the two shortings for the top metal frame. The study of the variations on the return losses in function of distance d and location L (seen in Figure 3 (c)), shows that the position of the shorting portion number 1 does not largely affect the impedance bandwidth but it affects the input matching at the resonance frequency (1575MHz) (Figure 4 (a)). Therefore, this parameter can be left variable for last-minute adjustments.

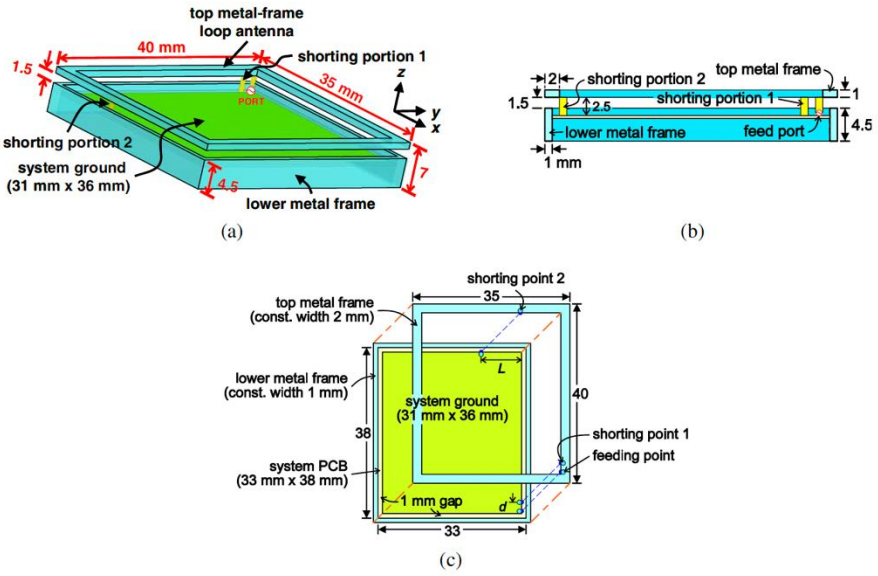

Figure 3: (a) Perspective drawing of the proposed GPS loop antenna integrated into the top metal frame of a smartwatch. (b) Sectional view of the top metal frame, the low metal frame, and the system PCB. (c) Top view of the proposed design

On the other hand, parameter L has a higher influence on the resultant resonation frequency from the antenna (Figure 4 (b)). Finally, the optimal value for the L parameter has been set to 8.5mm, allowing the metal-frame antenna to be resonant at 1575MHz.

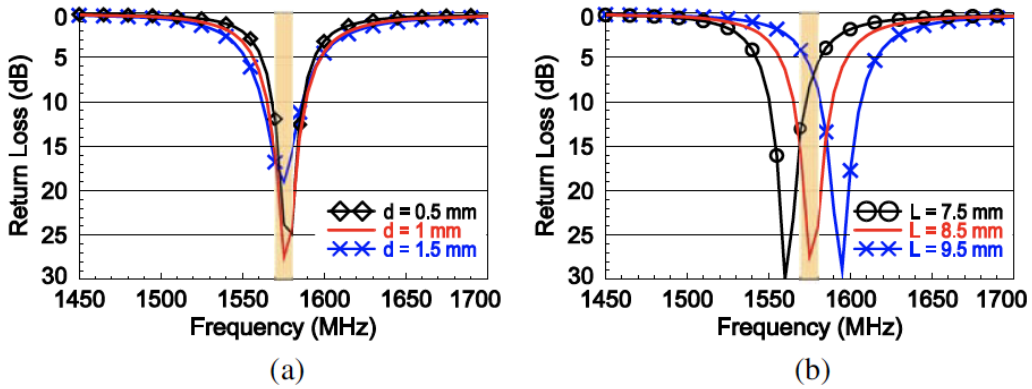

Figure 4: Simulated return losses for the proposed antenna as a function of (a) the distance d and (b) the location L of the two shorting portions.

In addition, the proposed design has been also studied taking into account the impact of the human hand and forearm (Figure 5). Results show that, although the peak gain decreases, return loss is still better than 7,3dB at the resonance frequency.

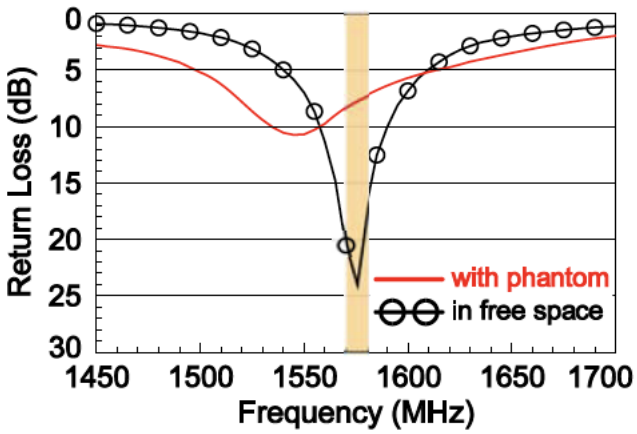

Figure 5: Measured return losses for the proposed design with the user's forearm and hand phantom and for the antenna in free space.

2.2.2 Antenna Designs of Smart Watch for the Cellular Communications by using Metal Belt

In this scientific paper [6] three different antenna models are introduced. All three designs enlarge the antenna's PCB by attaching cooper tape in the watch's rubber band (Figure 6). The first is based on a dipole mode (Figure 6 (a)), and the two other designs are based on a monopole (Figure 6 (b) and (c)).

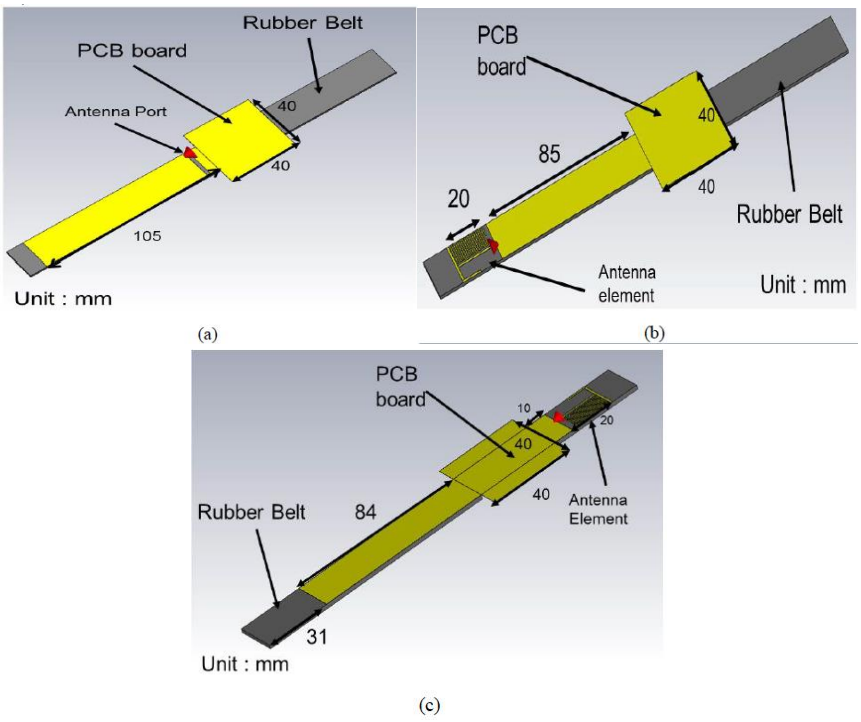

Figure 6: Antenna Structures of (a) Dipole antenna (b) monopole antenna 1 and (c) monopole antenna 2

When looking at the S_{11} parameters for all these three designs (Figure 7), the dipole shows the best performance in terms of matching, being able to operate from 700MHz to 960MHz and from 1700MHz to 2100MHz, which can cover almost all cellular bands.

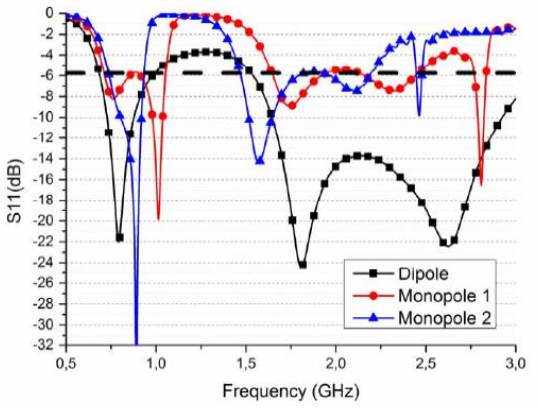

Figure 7: Simulated S11 for all three proposed designs

As this antenna is designed for a wearable, the effects of a human hand have been simulated in order to see which of the three proposed models best adapts to it.

The simulation shows (Figure 8) that the dipole model is the less stable one, being the most sensitive to deformation. The monopole-based prototypes show more robustness to the phantom hand.

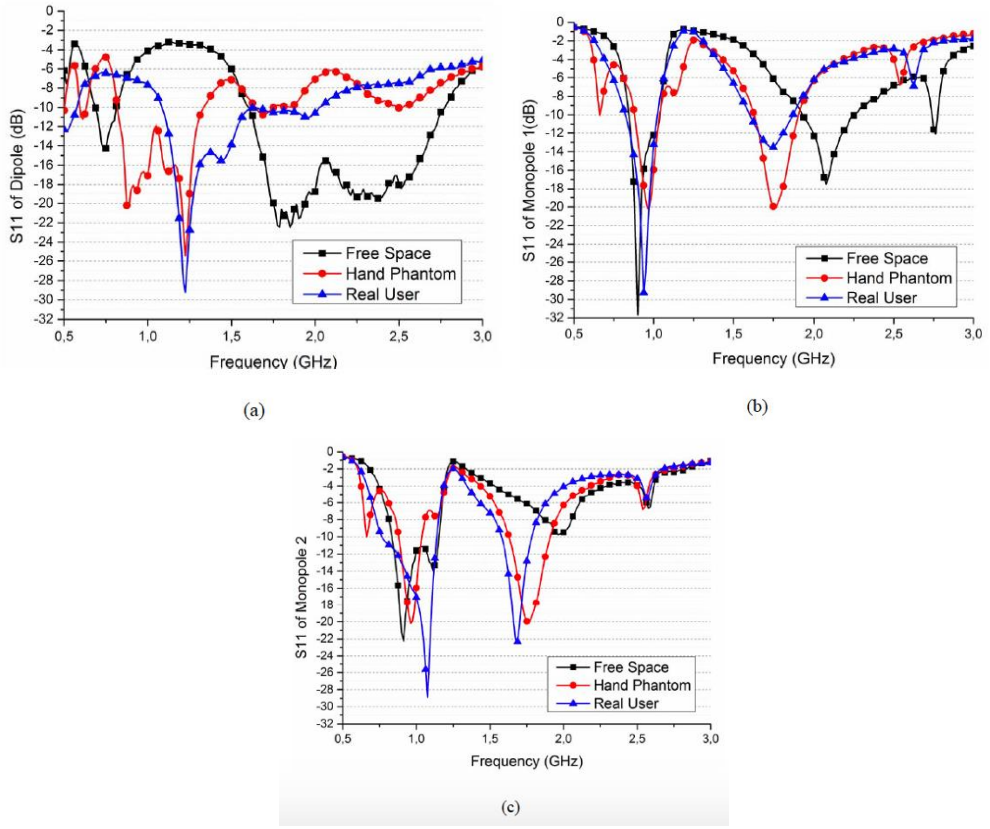

Figure 8: Measured antenna S11 of (a) the dipole antenna (b) monopole 1 and (c) monopole 2 in Free space, hand phantom and real user case

2.2.3 A Low-Profile Wearable Antenna Using a Miniature High Impedance Surface for Smartwatch Applications

This scientific paper [7] proposes using a miniature High Impedance Surface (HIS) for smartwatch applications.

The main idea is to use HIS to fight against the human body effect. However, HIS are usually too large. This study designs the most compact HIS structure to the date, making it fit in a resultant antenna of dimensions 38mm x 38mm x 3mm.

Table 1: Summary of the dimension, directivity, the number of unit cells, and SAR value of the literature.

No.	Dimensions (mm^3)	Number of Unit Cell	Directivity (dBi)	SAR Value
[8]	62 × 42 × 4	2 × 2	6.2	0.66
[9]	66 × 66 × 3.3	3 × 3	4.8	0.683
[10]	125 × 100 × 7.7	3 × 6	10.7	N/A
[11]	72 × 72 × 11	6 × 6	6.2	78
[12]	120 × 120 × 4.5	3 × 3	6.4	0.079
[13]	100 × 120 × 7.2	6 × 5	7.1	N/A
[14]	110 × 130 × 3.9	8 × 8	5.1	N/A
This work	38 × 38 × 3	2 × 2	6.3	0.29

Table 1 shows the state of the current literature to what HIS refers (original references can be found at the complete article). Thus, up to this point the smallest volume for a smartwatch antenna with a finite-sized HIS (at 2440MHz) is 62mm x 42mm x 4mm.

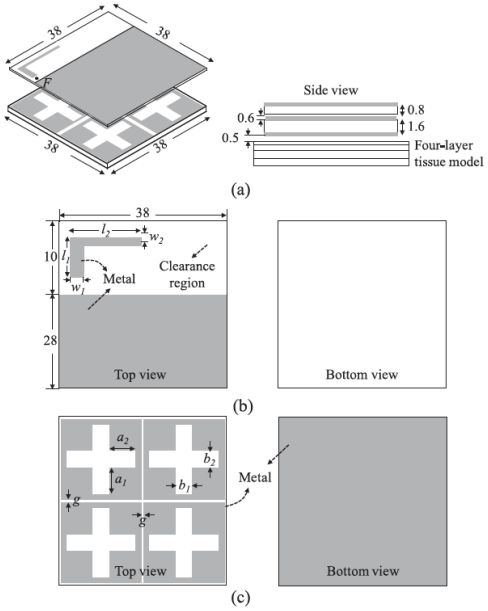

Figure 9: (a) Configuration of the proposed integrated antenna. (b) Top and bottom views of the top ILA. (c) Top and bottom views of the finite-sized HIS (Unit: mm).

The proposed design (Figure 9) reduces the smallest structure to the date by 45.5% and achieves good enough performance results (Figure 10) in high frequencies, even when placed on wrist.

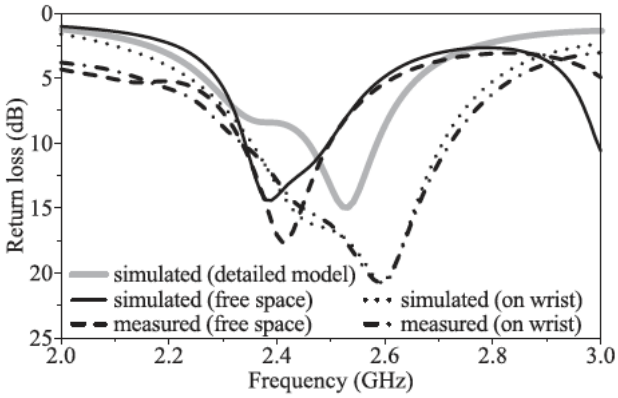

Figure 10: Simulated and measured return loss of the integrated antenna placed in different environments.

2.2.4 MIMO Antenna with Wi-Fi and Blue-Tooth for Smart Watch Applications

This reading [8] proposes a WiFi and Bluetooth, MIMO type antenna. This antenna (Figure 11) has been fabricated using a FR4 substrate with 0.4mm of thickness, relative permittivity of 4.4 and loss tangent of 0.024. Its dimensions are 40mm x 40.2mm x 5.4mm, containing two IFA antennas and a plane ground. The IFA type antennas excite the 2400MHz resonant mode.

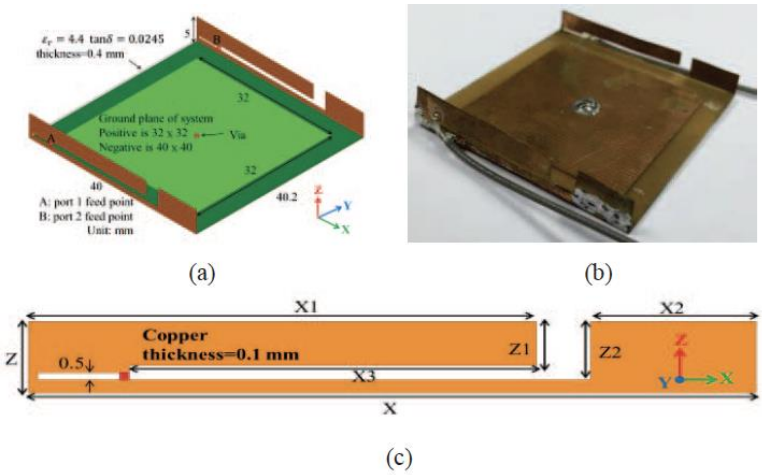

Figure 11: (a) The geometry of the proposed antenna, (b) Photograph of a fabricated antenna design, and (c) Detailed parameters of the IFA antenna.

In order to emulate more realistic conditions, an ABS shell and a screen have been added to the design. Results show (Figure 12) that by adjusting the X1 value for the IFA antennas, the resulting antenna is able to operate at both Bluetooth and WiFi bands.

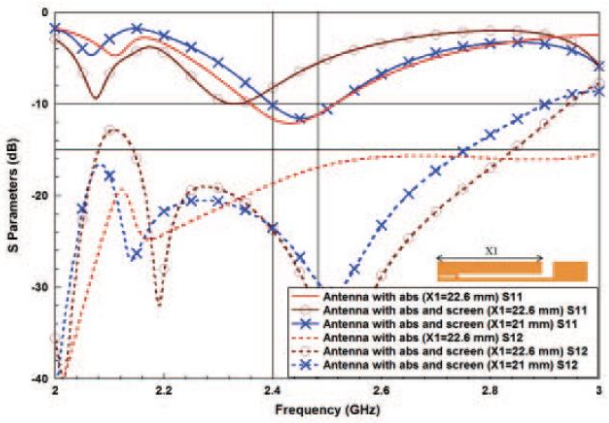

Figure 12: Simulated S11 of the proposed antenna with ABS and screen

2.2.5 Slot Antenna for All-Metal Smartwatch Applications

This article [9] introduces a circular slot-antenna for smartwatches for 2400MHz Bluetooth and WIFI applications. As usually in this kind of studies, the effect of the human hand has been simulated with the addition of a phantom arm.

The proposed antenna (Figure 13) has been though to fit an all-metal smartwatch. In this study, the proposed design has not been implemented but simulated.

The bottom arc-shaped slot, with a length of $3\lambda/4$ in free-space at 2450MHz, represents the proposed slot antenna.

One of the pros for this design is that, since the slot antenna is part of the smartwatch body, there is no need to add an individual antenna, making the cost decrease as long as the complexity.

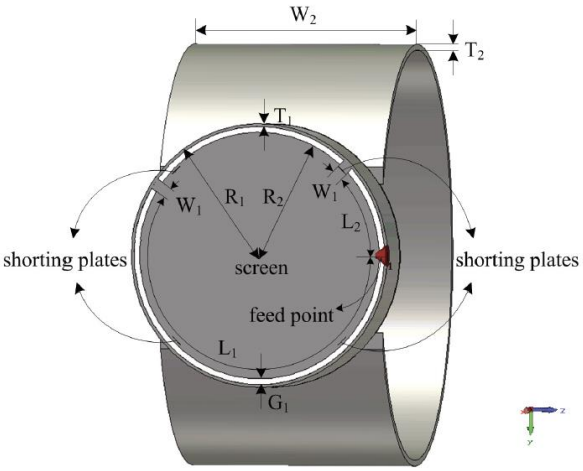

Figure 13: Geometry of proposed smartwatch antenna

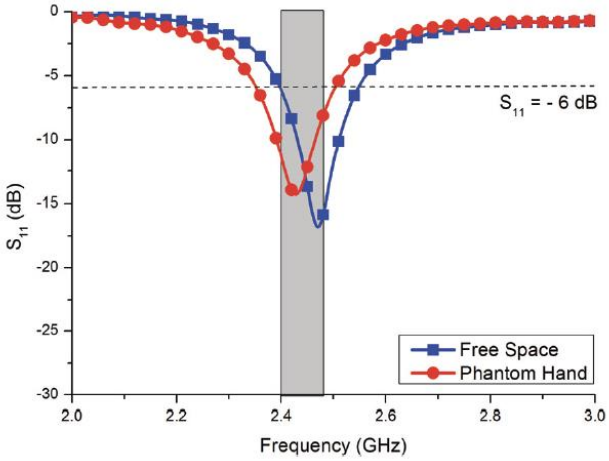

Figure 14: Simulated S11 of proposed smartwatch antenna.

Both the Free Space and the Phantom Hand simulations (Figure 14) show a more than enough good behaviour from this antenna on the interest frequencies.

As long as this model has not been implemented and tested, results may vary when materializing it. Nevertheless, the obtained results show that this antenna is capable of covering the Bluetooth and WIFI bands.

2.2.6 Conformal Bluetooth Antenna for the Watch-Type Wireless Communication Device Application

This scientific paper [10] main purpose is to study the effect of the human hand and forearm to wearable device's antennas radiation efficiency. The chosen antenna is a T-shaped monopole, with a low profile of 4mm.

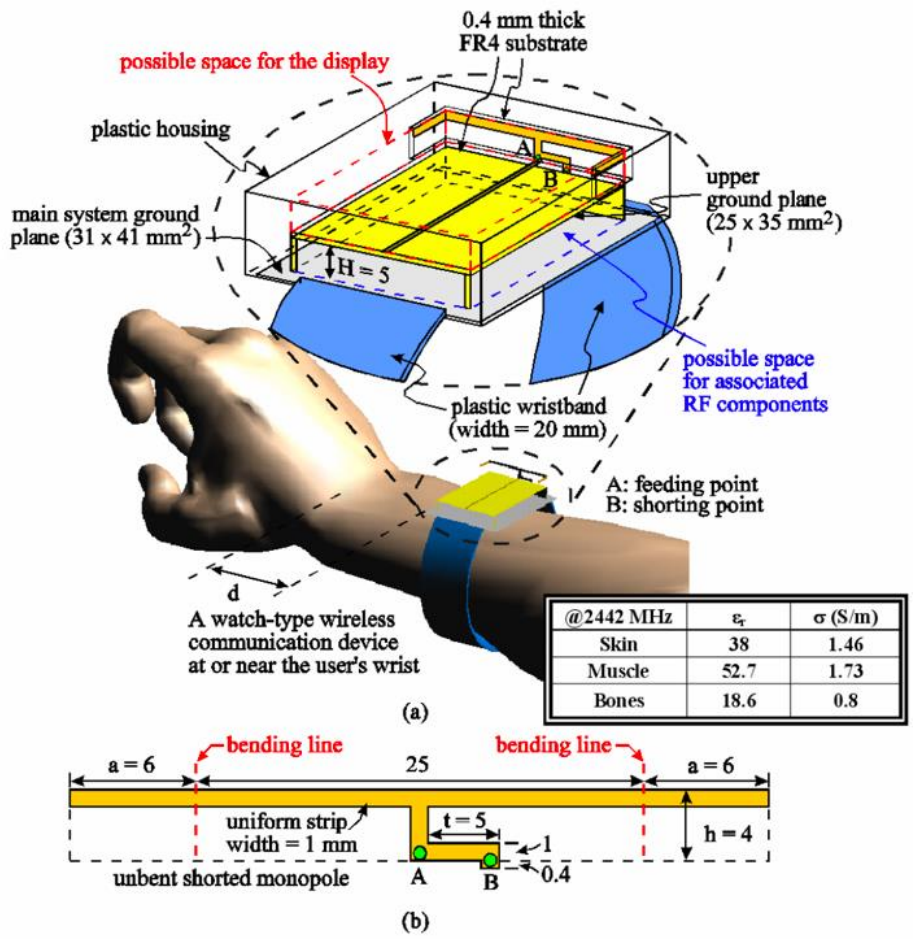

Figure 15: (a) Configuration and simulation model of the watch-type wireless communication device with the conformal Bluetooth antenna. (b) Detailed dimensions of the antenna.

As shown in the designed model (Figure 15), the T-shaped antenna is short-circuited to an upper ground plane. This secondary ground plane is at an H distance from the main system's one, which is supposed to be in contact with the human forearm. Thus, H is finally the distance between the antenna and the human forearm.

In order to study the effects of human skin, muscles and bones, the main two elements taken into account are distances H and d, being d the distance between the device and the start of the human hand.

Results show (Figure 16 (left)) that parameter d has a very low, and almost depreciable, effect on the return losses of the antenna. On the other hand, distance H has a high effect on the radiation efficiency (Figure 16 (right)), making it decrease from its initial value of 82%, obtained in free space, to a 50% when placing the antenna 5mm above the forearm.

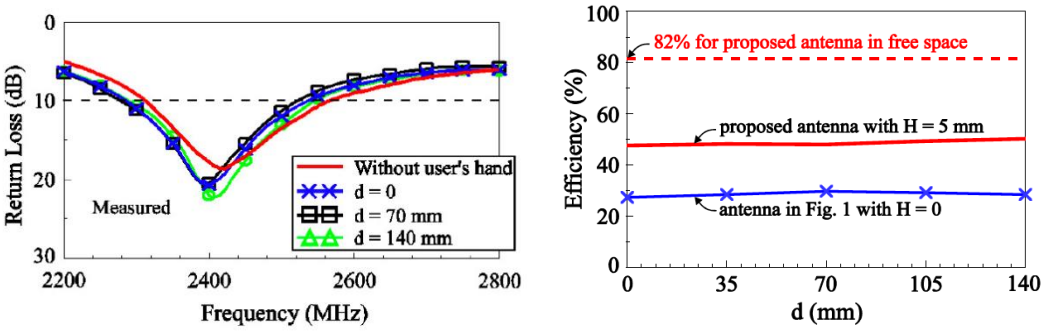

Figure 16: (left) Measured return loss for antenna with and without the user's hand and the experimental photo of the device. (right) Simulated (SEMCAD) radiation efficiency at 2442 MHz versus d for the antenna with H = 5 mm and 0.

2.2.7 Wearable Antenna Design on Finite-Size High Impedance Surfaces for Smart-Watch Applications

In this scientific paper [11] , an efficient technique based on the suspended microstrip-line method for characterizing the finite-size HIS structure Is proposed.

Conventionally, a conductive ground plane is used for wearable antennas due to the unidirectional radiation it offers. The problem is that those ground planes need antennas to be at a distance of a quarter wavelength from the back conductor, making the space it needs bigger. Replacing the ground plane by a HIS solves this problem, allowing antennas to be placed directly above the HIS. Nevertheless, HIS characterization has always been based on infinite, periodic unit-cell simulations, fact that conflicts with the compact available region defined for wearable antennas.

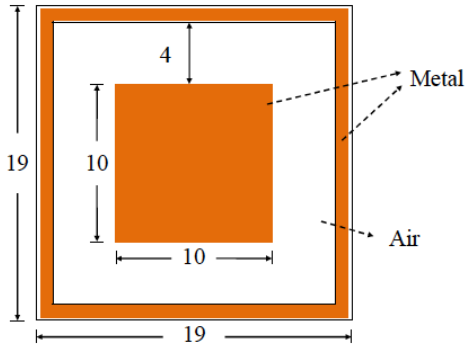

Figure 17: Geometry of the unit cell (unit: mm)

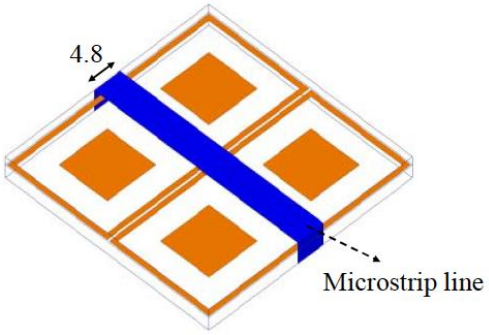

Figure 18: A suspended microstrip line over the HIS (unit: mm).

In this scientific paper, a 2x2 array patch (Figure 18) is studied. The 50Ω microstrip line connects ports 1 and 2. According to the theory of electromagnetic gap band (EGB), the structure rejects power transmission between ports 1 and 2 at the stop band (low S_{21} value). In the studied case, the stop band translates in the operation band.

Results show (Figure 19) that, defining interest frequencies as those with $|S_{21}|$<-20dB and $|S_{11}|$>-3dB, the proposed design is valid for working between 2400MHz and 2480MHz, meeting that way the design goals.

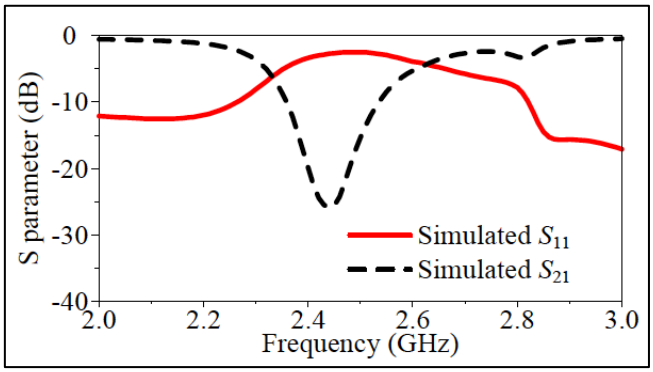

Figure 19: Simulated S parameters of the suspended microstripline characterization.

2.3 Conclusions

After reviewing the previous articles, the first idea that comes into mind is that there is still a lot to investigate in the field of smartwatches antennas. Many problems have been faced in those articles, such as the antenna dimensions, the ground plane, the integration with the watch case or the separation from the human forearm and hand.

Anyway, some conclusions can be withdrawn:

- Dimensions: Designed antennas for smartwatch applications must be compact and low-profile. Although it can seem obvious, it turns out as a complication when designing. Therefore, not only ground planes but also matching networks and antennas must be miniaturized in order to fit in a realistic-sized case, which has to be wearable comfortably.

  For this, looking at the actual market's offer and choosing a specific model to base the design in could be the best idea before starting to design a new model.

- Ground plane: In some of the previous articles, the idea of replacing a conventional ground plane with a finite HIS is debated. This idea can be suitable for a new project in which the available space is reduced. Another option shown in the read papers, is to enlarge the ground plane with cooper tape along the smartwatches rubber band.

In conclusion, the election of the ground plane format and size is one of the most important decisions to take when designing a smartwatch antenna model, being a must to study before selecting the definitive option. This is particularly relevant as far as low bands are concerned such as those in 698Mhz-906MHz frequency region-Integration with the watch case: Although many actual studies have successfully integrated the antenna in the metallic frame of the device, this design does not leave many options to modify and adapt the antenna. Nevertheless, it can be a good option for just operating with Bluetooth and WIFI.

- Effect of human body: If a ranking was made, this concept would for sure be in the top 3 in terms of importance when designing an antenna for a wearable device. As seen in many scientific papers, the human hand and forearm have a really big impact on the radiation efficiency; thus, it seems a good idea to separate the ground plane from the wrist/forearm a few millimetres, because it can improve the antenna's performance by at least a 20%.

3 Design and simulation

3.1 Introduction

Along this chapter, several prototypes will be designed and simulated, in order to obtain a certain number of candidates to proceed with the implementation.

For all the proposed models, the used technology will be the Antenna booster Antenna designed by Fractus [12] - [38] .

3.2 Finding the optimal ground plane dimensions

The first step of the design is to find the optimum size for the ground plane. As seen in the previously discussed literature, this will be one of the main aspects that will determine the future behaviour of the whole antenna.

To do so, the initial design is composed of a 30 x 30 mm^2 ground plane and a 3 mm x 12 mm x 2.4 mm Antenna booster. Below the ground plane, there is a dielectric layer of 1mm. There is also a port between the ground plane and the connection track with the GPB (Figure 20).

This initial model has been modified in many different ways, getting closer to the real case at every step, and the resulting models have been adapted in order to obtain their bandwidth at the interest frequencies.

All proposed models have been designed with the IE3D software and simulated and matched with the MicroWave Office software.

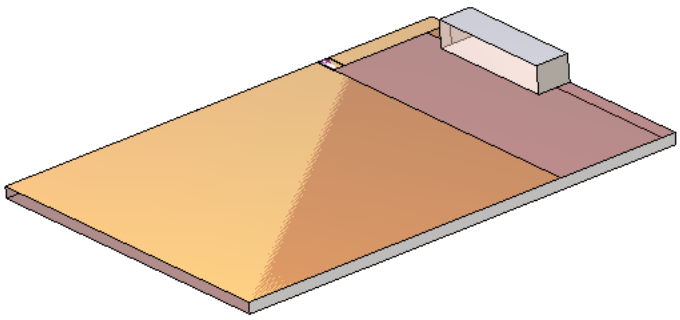

Figure 20: Original 30 x 30 mm^2 ground plane with an integrated Antenna booster

3.2.1 First designs

To start with the search of the optimum size and shape of the ground plane, a straight and a completely circular enlargements have been designed and simulated. Those two designs will indicate the path to follow for the next stages in the reach of the final candidates.

3.2.1.1 Straight enlargement at free space

Starting from a 30 x 30 mm^2 ground plane, with an integrated GPB, the design has been enlarged to 30 x 60 mm^2, 30 x 90 mm^2 and 30 x 120 mm^2. For this model, its behaviour around de GSM band, centred at 900MHz, has been studied at free space.

The frequential bandwidth has been calculated in percentage as follows:

Equation 1: Frequential bandwidth computation

$$BW(\%) = \frac{f2 - f1}{(f2 + f1)/2} \cdot 100$$

being f_1 and f_2 the lower and upper frequencies at -6dB for the antenna's return losses respectively.

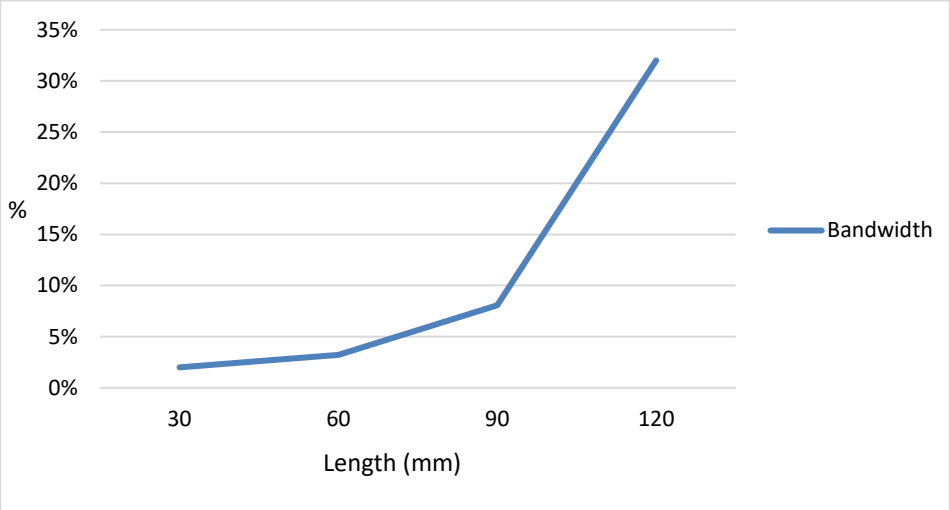

Figure 21: Antenna's frequential bandwidth as a function of the ground plane length

Table 2: Resulting bandwidth after adapting the original and the enlarged models to 900MHz

Ground Plane Dimensions	BW (MHz)	BW (%, SWR=3)
30 x 30mm^2	18MHz	2.0%
30 x 60mm^2	29MHz	3.2%
30 x 90mm^2	73MHz	8.0%
30 x 120mm^2	309MHz	32.0%

Results show (Table 2 and Figure 21) that the larger the ground plane the wider the resulting bandwidth, reaching a maximum of 32% for the 30 x 120 mm^2.

Furthermore, the width of the enlargement has also been studied in order to know its effect on the previous results. This way, the 30 x 90 mm^2 (60mm enlargement) model has been studied again, but this time reducing the enlargement width to 10 and 20 mm. As seen in the results (Table 3), the obtained bandwidth does not suffer many variations, meaning this that, in a future, narrower enlargements can be used if necessary.

Table 3: Study of the effects of the enlargement width

Enlargement dimensions	BW (MHz)	BW(%, SWR=3)
10x60mm^2	75MHz	8,32%
20x60 mm^2	78MHz	8,65%
30x90 mm^2 (from Table 2)	73MHz	8,07%

3.2.1.2 Completely round enlargement at free space

In this section, the same study as in the previous case has been done, but this time the ground plane enlargement is circular. This is necessary because, in the case of implementing this design, that enlargement would be implemented as a cooper tape inside the watch belt, and so it would be circular.

For this study, a 150mm long wrist has been supposed, the ground plane has been increased with 30, 60 and 90mm of extra cooper (**Error! No s'ha trobat l'origen de la referència.**) and the adaptation has been done both at 900MHz (GSM band) and 1800MHz HF).

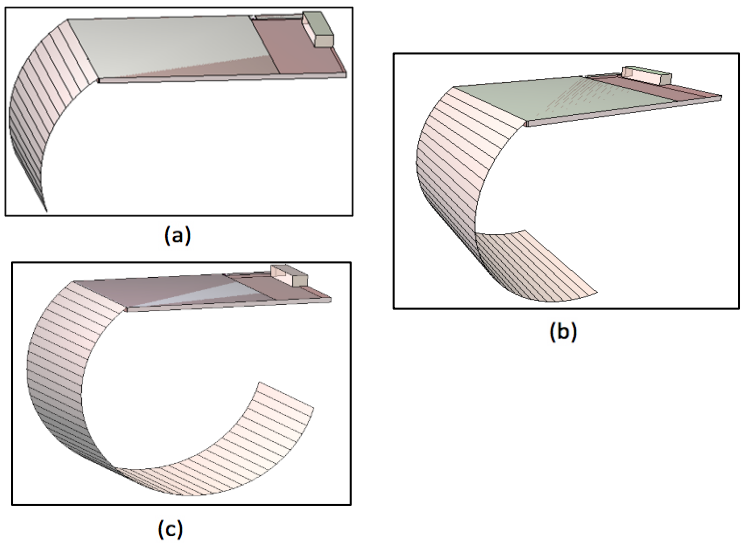

Figure 22: Ground plane enlargements in a circular shape. (a) 30mm; (b) 60mm; (c) 90mm

After adding the proper matching network to every design to make them resonate at 900MHz (Figure 23) and 1800MHz (Figure 24) respectively, results (Table 4) tell that the fact of giving the enlargements a round shape has a negative impact on the achieved bandwidth in comparison of the obtained results for the straight enlargements (3.2.1.1).

Anyway, and studying these results independently, it has been proved that the resulting bandwidth improves as larger the ground plane is, consolidating the conclusions from the previous section (3.2.1.1): the larger the ground plane, the wider the bandwidth at the interest frequencies.

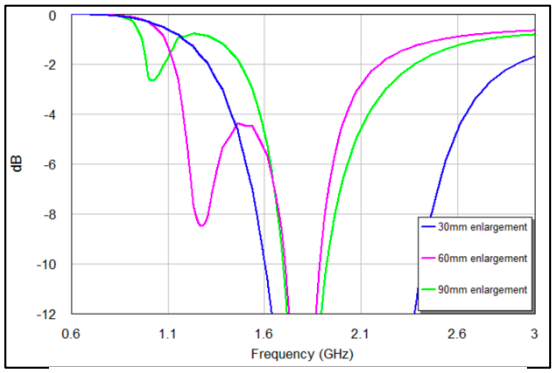

Figure 23: Return losses for the proposed designs at 1800MHz

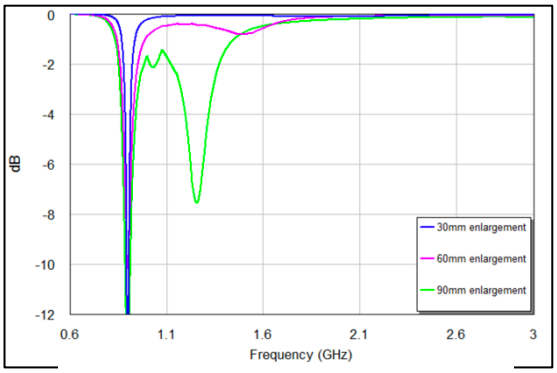

Figure 24: Return losses for the proposed designs at 900MH

Table 4: Comparison between the bandwidth and the frequential bandwidth at 900MHz and 1800MHz for all the proposed designs

Enlargement length	@900MHz (Bandwidth / Frequential BW)	@1800MHz (Bandwidth / Frequential BW)
0mm	18MHz / 2%	210MHz / 11.6%
30mm	30MHz / 3.3%	1.04GHz / 51.5%
60mm	39MHz / 4.3%	340MHz / 19%
90mm	70MHz / 7.7%	400MHz / 21.8%

3.2.2 Wrist-shaped design at free space

In this section, starting from the acquired background from the previous one (0), a more realistic design is proposed. In this case, the previous round design is adapted so it is closer to the shape of a worn watch.

Thus, a deeper study has been done, and more lengths for the enlargement have been designed and simulated.

3.2.2.1 Base model and 30mm extension

As in the previous case, the base model is a 30 x 30 mm^2 ground plane (Figure 20). After adapting it to be resonant at 900MHz (Figure 25) the resulting bandwidth at -6dB goes from 895MHz to 905MHz making a total of 10MHz.

Looking now at the 30mm extended model, which has a very similar shape than its homologous (**Error! No s'ha trobat l'origen de la referència.** (a)), it can be seen (Figure 27) that the little differences on its belt curvature have made it lose 7MHz of bandwidth (from the previous 30MHz to this model's 23MHz).

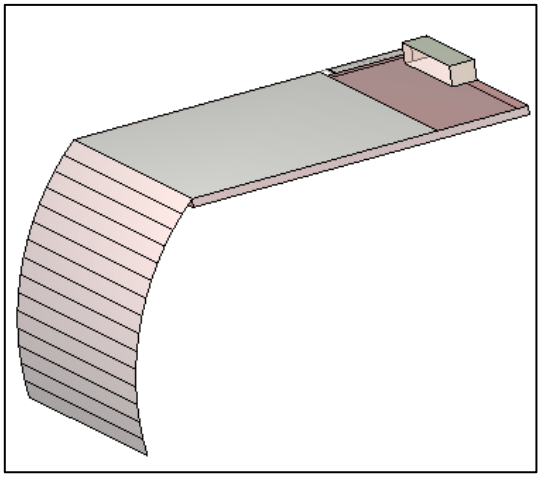

Figure 26: 30mm enlarged model

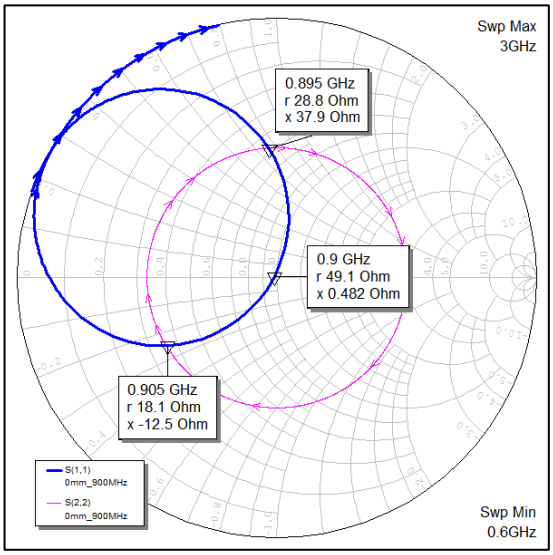

Figure 25: No extended model return losses at 900MHz

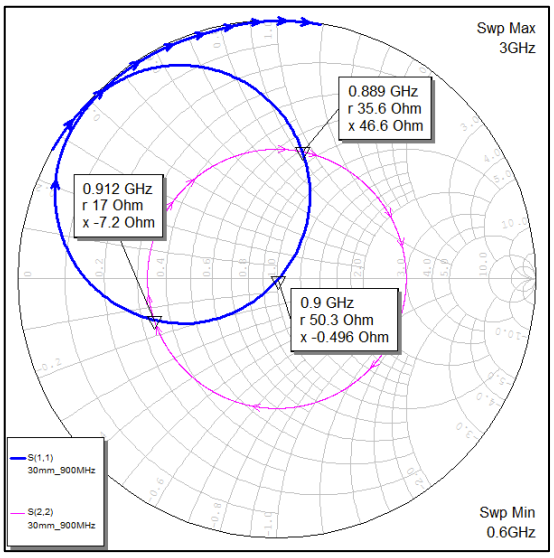

Figure 27: 30mm extension model return losses at 900MHz

3.2.2.2 60mm and 90mm extension

In this models, two main differences comparing to their predecessors will be noticed. The first one is in the shape, where the curvature makes an angle leading to the “flat lower part of the wrist” (Figure 28).

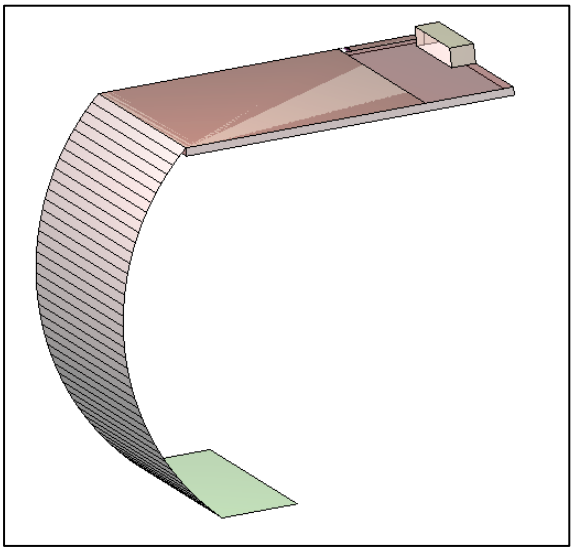

Figure 28: 60mm enlarged model

Moving now to their return losses, yet in the first of these models a small perturbation in the curvature can be observed (Figure 29). In the following designs, this loop will grow, and advantage will be taken from it trying to make it stay below -6db and so getting a wider bandwidth in return.

Apart from that, the 60mm enlargement does not show a big improvement in the resulting bandwidth, reaching a total of 36MHz below -6dB.

Looking at the 90mm enlarged design (Figure 29), the commented loop is clearly seen. Even so, in this case the frequencies included on the loop are not below -6dB and the resulting bandwidth has not improved enough yet, achieving only 61MHz (25MHz more than in the previous case).

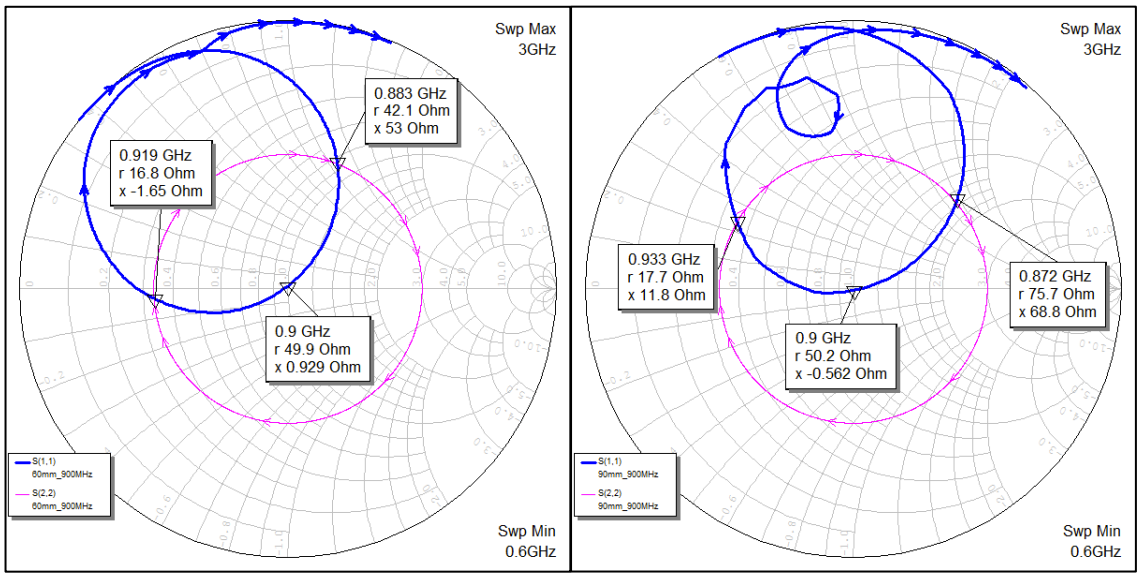

Figure 29: Return losses presented in a smith chart for the 60mm (left) and the 90mm (right) enlargements

3.2.2.3 100mm, 110mm and 120mm enlargements

In these models, the bandwidth below -6dB increases significantly. This is due to the frequential loop being inside the SWR 3 circle. Thus, these models present wider enough bandwidths to be considered as candidates for further studies.

Looking at their resulting smith charts when adapted to be resonant at 900MHz, the loop is seen inside the SWR 3 circle:

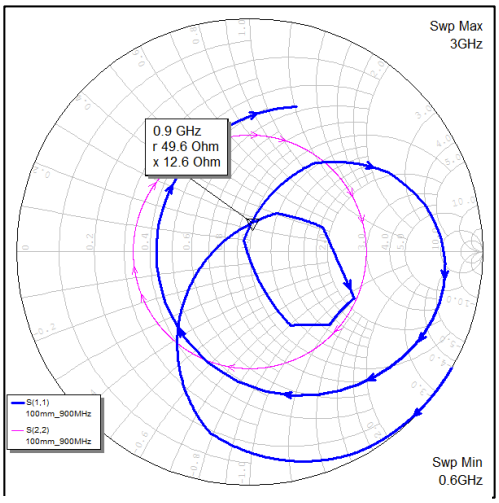

Figure 31: 100mm extension return losses when adapting @900MHz

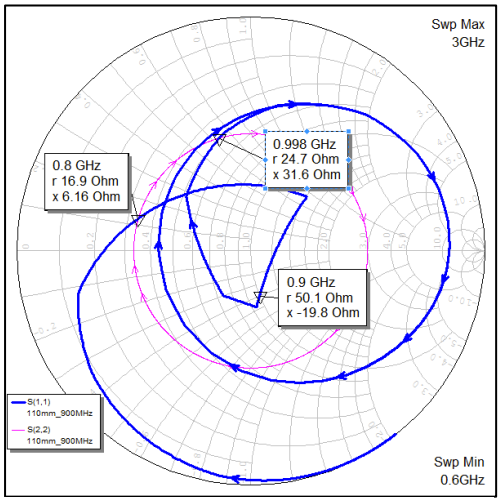

Figure 30: 110mm extension return losses when adapting @900MHz

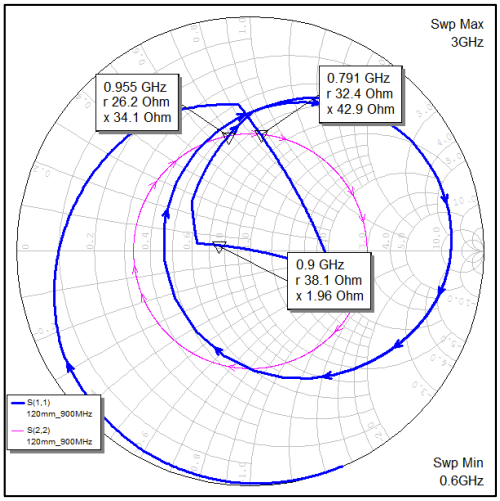

Figure 32: 120mm extension return losses when adapting @900MHz

3.2.2.4 Results

To sum up the previous presented models, Table 5 shows every case's starting and ending frequencies between which S_{11} is below -6dB, and also the total bandwidth both in MHz and in percentage.

As seen in the previous paragraphs, it is not until the 100mm extension where the bandwidth is large enough to properly work at the interest frequencies. Then, this study lets as the best candidate the 110mm extended model. Although its resulting bandwidth is a 7% shorter than in the 100mm extension case, the start frequency for this case makes it cover the GSM-850 and the GSM-900 bands as long as many LTE bands.

Therefore, considering this wrist-shaped design and free-space, the final candidate to be implemented would be a 30 x 30 mm^2 ground plane extended with 110mm of more conductive surface.

Table 5: Wrist-shaped designs resulting bandwidths at 900MHz

Model	F1	F2	Bandwidth (MHz)	Bandwidth (%)
Original	895MHz	905MHz	10MHz	1.1%
30mm extension	889MHz	912MHz	23MHz	2.5%
60mm extension	883MHz	919MHz	36MHz	4%
90mm extension	872MHz	933MHz	61MHz	6.7%
100mm extension	866MHz	1160MHZ	294MHz	29%
110mm extension	800MHz	998MHz	198MHz	22%
120mm extension	791MHz	955MHz	164MHz	18.8%

3.2.3 Wrist-shaped design with phantom forearm

In this chapter, the models from 3.2.2 are taken again but a simulated human forearm is included to the study. The human hand has not been included due to its small effect on the antenna's return losses, as seen in the reviewed lectures.

3.2.3.1 Base model

The base model for this chapter is the previous 30 x 30 mm^2 ground plane with a 150mm long phantom forearm (ε_R = 5; σ=0,013).

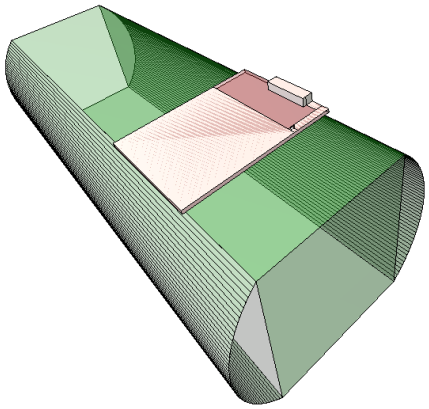

Figure 33: 30 x 30 mm^2 ground plane with an added phantom forearm

As learnt in chapter 2, the presence of the human forearm is the factor which most effects to the behaviour of the antenna. In this particular case, the resulting S11 (Figure 34) shows a resulting bandwidth of 120MHz. At a first sight, one can think that the situation has drastically improved, taking in account that without the phantom forearm the same model had a 10MHz bandwidth. As will be shown later, the problem introduced by this new component comes when computing the radiation efficiency.

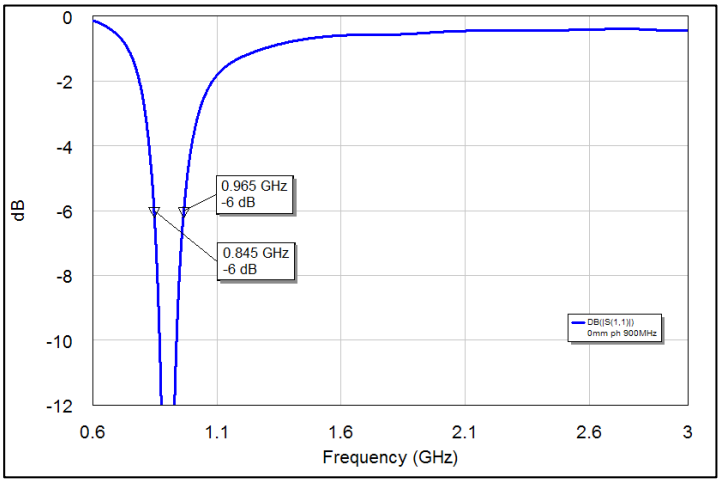

Figure 34: Return losses for the base model with a phantom forearm at 900MHz

3.2.3.2 Results

After repeating the steps from the previous section, every single model has presented a wider bandwidth with the addition of the phantom forearm (Table 6).

The model which performs the best in the goal frequencies is the one with a 90mm ground plane enlargement, reaching a total bandwidth of more than 850MHz. This same model at free space had a resulting bandwidth of 61MHz.

Table 6: Wrist-shaped designs resulting bandwidths at 900MHz with the addition of a phantom forearm.

Model	F_1	F_2	Bandwidth (MHz)	Bandwidth (Percentage)
Original	845MHz	965MHz	120MHz	13.2%
30mm extension	802MHz	1050MHz	248MHz	26.8%
60mm extension	628MHz	987MHz	359MHz	44.5%
90mm extension	<600MHz	1450MHz	850MHz	83%
110mm extension	664MHz	1500MHz	836MHz	77.3%
120mm extension	<600MHz	1360MHz	760MHz	77.5 %

Despite these results, the radiation efficiencies of all models have to be also studied before picking the final candidate. As explained in the introduction of this chapter, the phantom forearm has a huge effect on the antenna's radiation efficiency, as long as it is a barrier for the signal to spread.

In order to know how big is this phantom forearm' effect, the radiation efficiency for the previous case candidate (110mm of enlargement at free space) (3.2.2.4) has been computed (Figure 35).

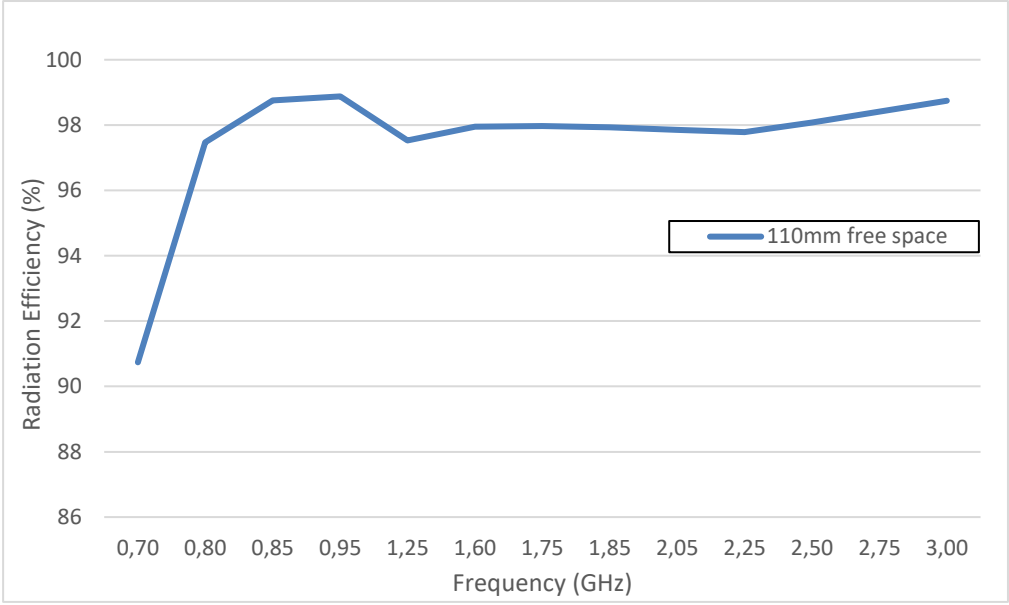

Figure 35: Radiation efficiency for the 110mm extended model at free space

This result shows a big antenna's radiation efficiency, being that value over a 90% in the whole spectrum.

Moving now to the models with a phantom forearm, the efficiency values decrease drastically (Figure 36). It can also be observed that, as a general rule, the longer the ground plane's enlargement is the lower the radiation efficiency becomes. The only exception comes in the 90mm extension case, in which the radiation efficiency stays almost equal that in the base case.

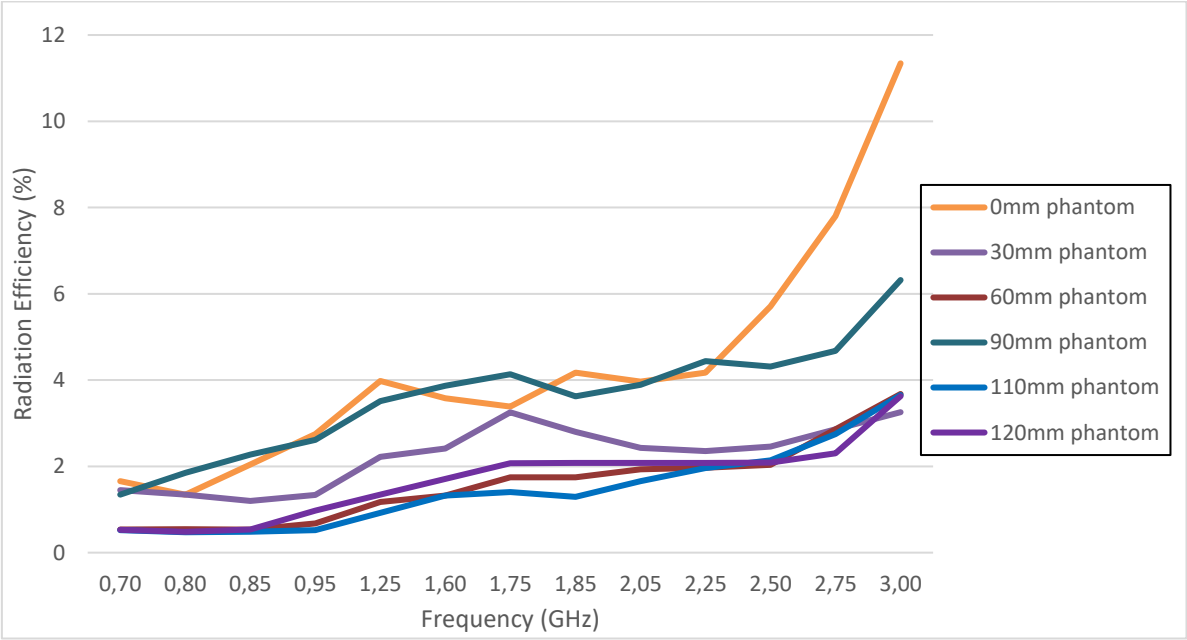

Figure 36: Radiation efficiencies for the proposed models with a phantom forearm

3.3 Conclusions

In this chapter, many different antenna models have been designed and simulated. The base model has been a 30 x 30 mm^2 ground plane, with a Antenna booster

This base model has been modified by extending it with different lengths, and all the models have been adapted to 900MHz. As the extensions are supposed to be attached to the watch's belt in case of being implemented, they have been designed first in a circular shape and later in a wrist shape.

Furthermore, a simulated phantom forearm has been finally added to the study, in order to measure its effect on the antenna's resulting bandwidth and radiation efficiency.

Finally, and after reviewing the previous results, the chosen candidate to be implemented in the following stages is the 90mm extended one. This model presents an 850MHz bandwidth at the GSM band and has a simulated efficiency close to the base model.

4 Prototype

4.1 Introduction

In this chapter, many different antenna models will be implemented and studied. Starting from the candidate in last chapter (3.3), different conditions and matching networks will be studied whiling to find a solution that fits the markets requirements.

All the tasks realized in this chapter have been done in the Fractus Antennas Headquarters laboratory. This working place counts with a chemical laboratory, an anechoic chamber and many signal analysers, as long as with all the necessary materials for manufacturing and studying an antenna.

Before this stage is started, it is important to review all the previous work done in order to have a clear idea of the pursued objective and to settle the steps to follow. The workflow for this stage can be summarized as follows:

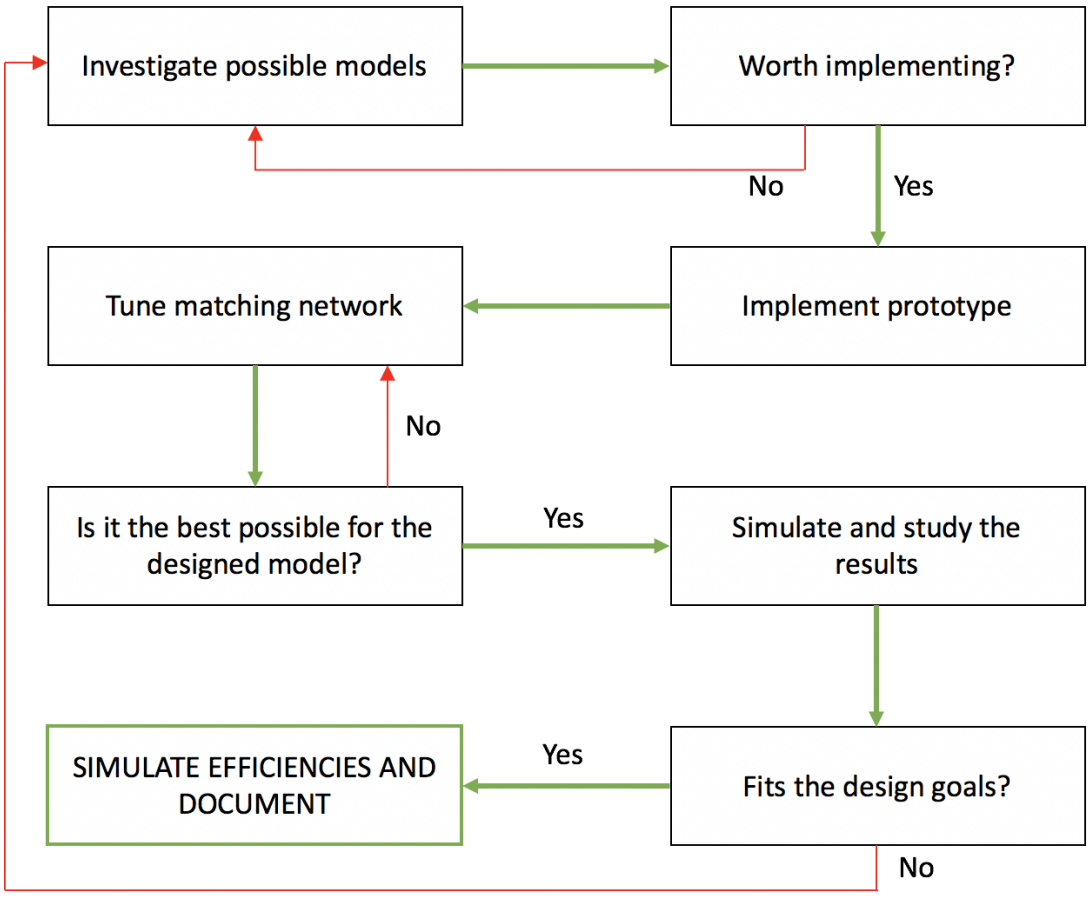

4.2 Objective

The objective of this chapter is to find a model capable of working at the GSM bands as long as in the HF. This means that the proposed models will be adapted so their return losses are below -6dB between 824MHz and 960MHz and between 1700MHz and 2170MHz.

4.3 Implementation

The first step for the construction of an antenna is to create the ground plane. Thus, it is necessary to design that ground plane with a CAD software and then print it in greaseproof paper (Figure 37).

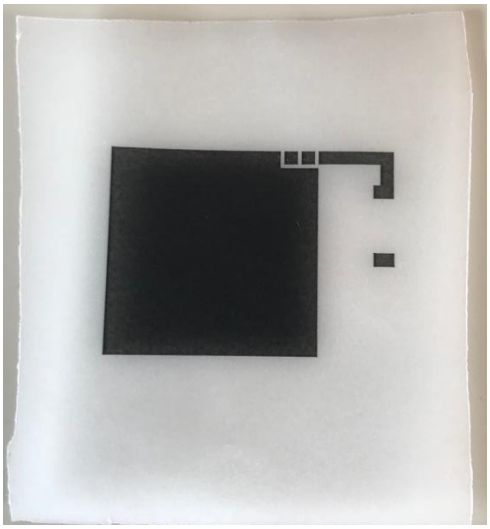

Figure 37: Printed ground plane design

The next step is to isolate for 3:30 minutes a FR4 board (ε_R= 4.15, tan(δ)=0.013) using the printed design as a mask.

Then, the board must be submerged into a positive revelator liquid. In this point, the designed shape will be visible in the cooper surface of the board.

To eliminate the undesired cooper from the board, an acid composed of salfuman (25%), hydrogen peroxide (25%) and water (50%) is used to submerge the board again.

Finally, when all the undesired cooper has left, the board is cleaned with acetone to eliminate any rests that may be on it, and a final wash with water is also applied.

Once the board has been manufactured, both the antenna booster and the feeder are incorporated, and the pads are short-circuited with 0Ω resistances (Figure 38). Also, a tin line has been welded in the board in order to incorporate an enlargement in the future.

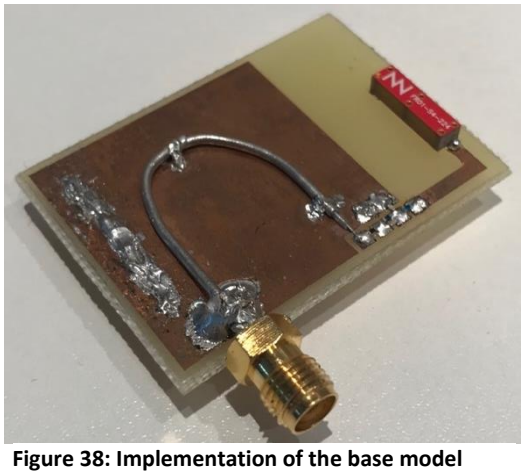

Figure 38: Implementation of the base model

The following step is to incorporate both the phantom hand and the 90mm extension (Figure 39). In order to implement the extension, a cooper tape has been attached to the watch's band. Then the S parameters are taken with the objective of designing a matching network for the antenna to work at the interest frequencies.

Figure 39: Base model with a 90mm extension and a phantom hand

4.4 Matching network

At first, a measure of the base model has been taken in absence of any matching network (Figure 40).

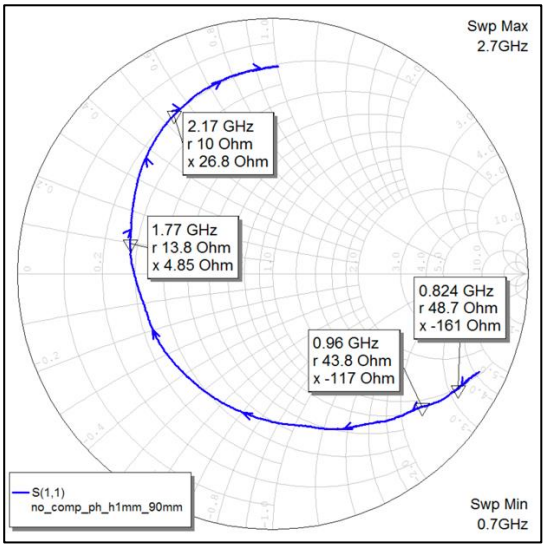

Figure 40: S_{11} for the base model in absence of any matching network

The objective is to place the frequencies included in the goal bandwidths inside the SWR-3 imaginary circle. Considering the different effects that condensers and inductors have, both in series and in parallel, to the high and the low frequencies from a spectrum, and considering the actual case, a matching network with two inductors and two condensers is proposed (Figure 41).

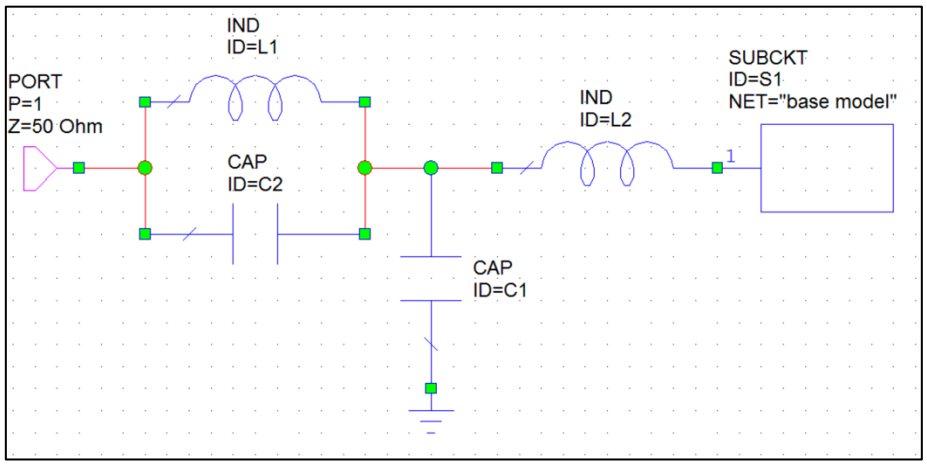

Figure 41: Proposed matching network

4.5 Models and measures

4.5.1 Procedure

In order to get the most adjusted value for every component, the optimizing tool available in the Microwave Office has been used. This tool allows setting as many conditions as wanted and then tries to accomplish them by tuning the different elements. In this case, the stablished conditions have been that for frequencies between 824MHz and 960MHz, and frequencies between 1770MHz and 2170MHz, the system S_{11} was below -6dB.

Once the optimizing tool ends computing the optimal value for every component, the closest to the Antenna booster is incorporated to the board and the S_{11} parameter is exported from the signal analyser. Back in the Microwave Office, a new optimization is done in order to see if, with the new real data incorporated, the rest of elements stay the same or suffer any variations. This process is repeated as many times as elements from the matching network can be independently studied.

4.5.2 Base model

The first model that has been studied is the resulting candidate from chapter 3.3. This means a 30 x 30 mm^2 ground plane with an integrated Antenna booster. The FR4 board used to print the design is 1mm thick, so this model is considered to be 1mm separated from the phantom hand. Also, a 90mm cooper band has been welded at the very ending of the board to extend the ground plane.

As explained in the previous point, the Microwave Office's optimizing tool has been used to design the optimal matching network values to reach the design goals. It can be seen (Figure 42) that the resulting matching network (Figure 43) provided by the optimizer tool would make this model fit the design requirements.

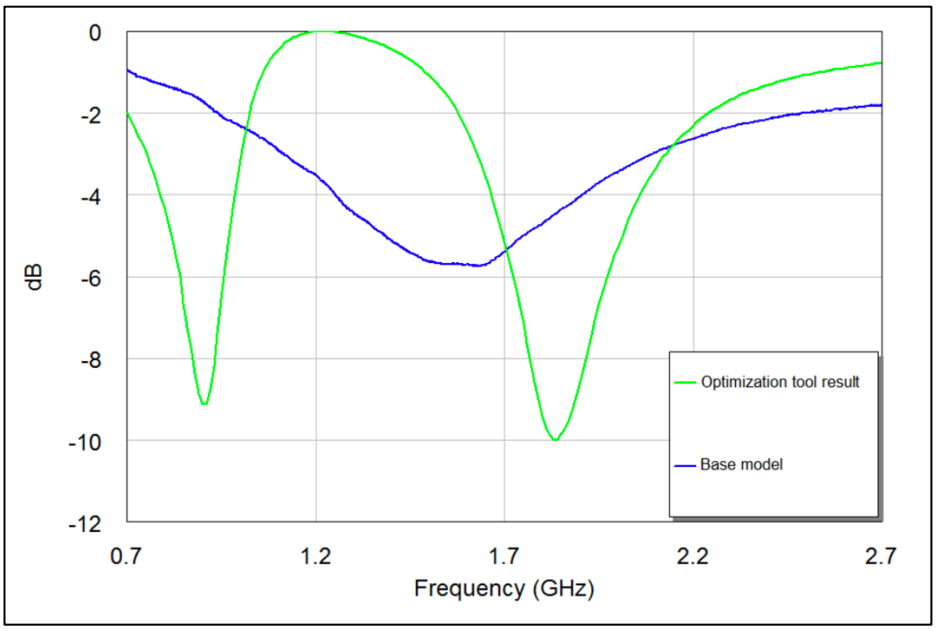

Figure 42: Comparison between the S11 parameters from the Base Model and the Optimizer Tool result

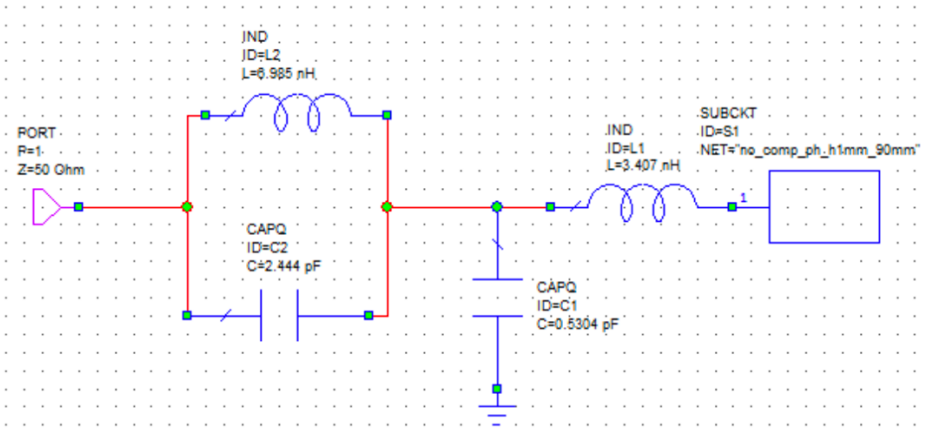

Figure 43: Resulting matching network provided by the optimizing tool

Unfortunately, neither the Optimizing Tool nor the Microwave Office consider some variations introduced by real components. Therefore, the whole proposed matching network is not applied and just the first element (L1) is welded instead. To know if the chosen value for that element has the proper effect on the circuit's return losses, a simulation with only that element is carried out (Figure 44) and the real element is changed until the best-fitting one is found.

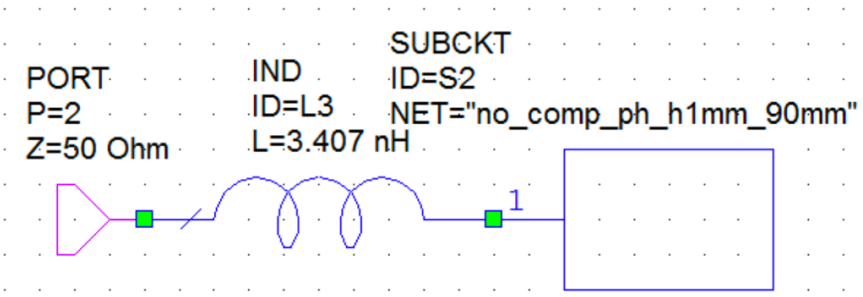

Figure 44: Circuit to compute L1's effect on the return losses

With this Inductor as the only element in the implemented matching network, the S_{11} values are extracted from the analyser and introduced back in the Microwave Office. Due to physical and circumstantial effects from the implemented element and the design's environment, even the L1 value that fits the best to the optimizer's purpose does not reach the exact effect on the return losses (Figure 45). It is then easy to figure out that, after all the elements are introduced, the accumulated error will make the resulting return losses differ from the expected ones.

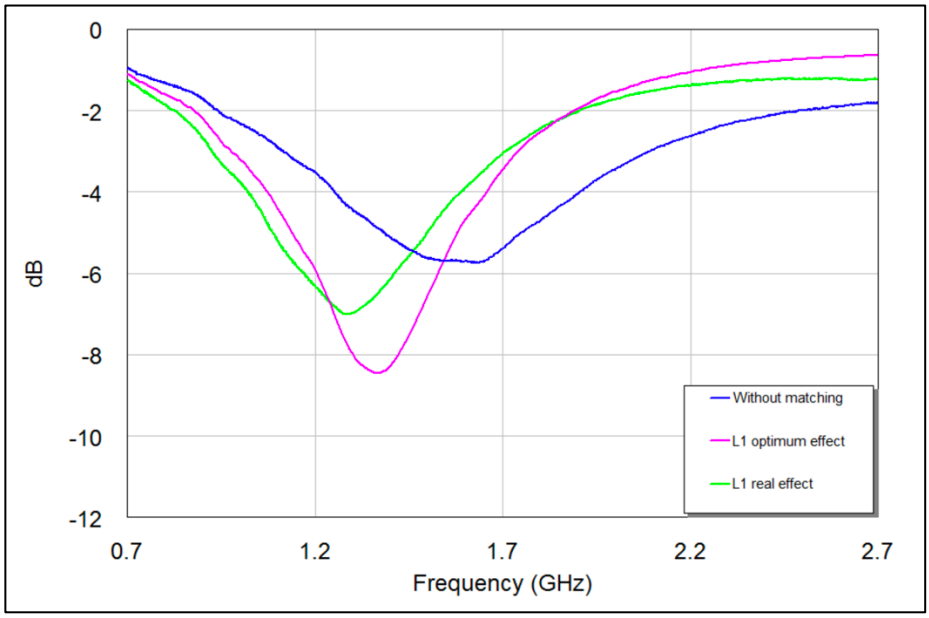

Figure 45: Comparison between L1 spectated effects and L1 real effects after implementation

Once the first element is welded, it is eliminated from the circuit (Figure 46) and the optimization is done again.

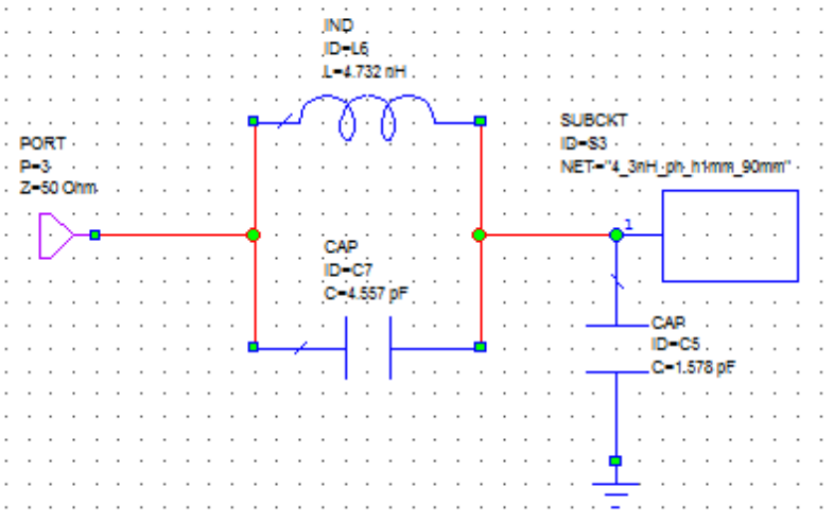

Figure 46: Resulting circuit after implementing L1 in the board and using that information to optimize the rest of elements again

At this point, the executed process for L1 is repeated to find the best possible value for C1, L2 and C2, and the final matching network implemented.

In order to understand how large the error introduced by the physical elements is, the evolution of the effect on the return losses of the optimum components (those resulting from the optimization tool) has been computed (Figure 47) and compared with the effect of the implemented elements (those resulting from the manual tuning) (Figure 48).

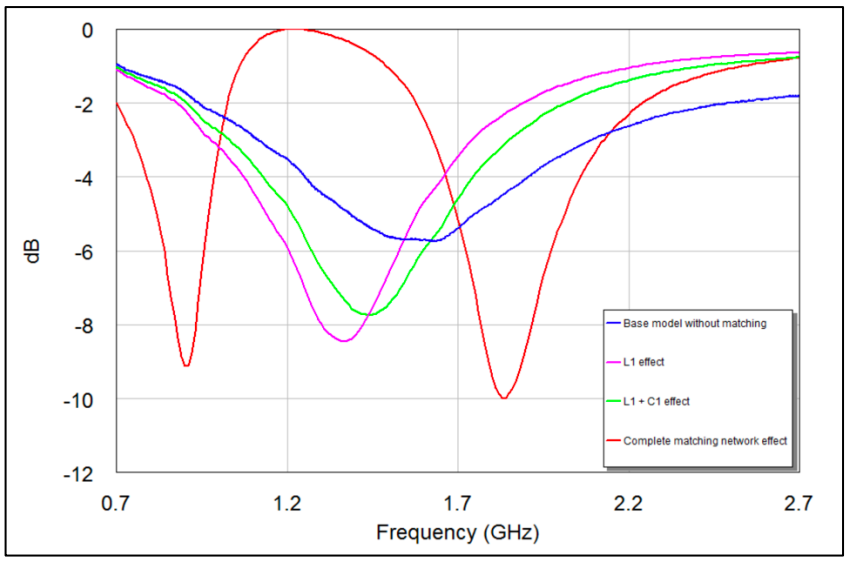

Figure 47: Evolution of the S11 after adding every optimized element to the matching network

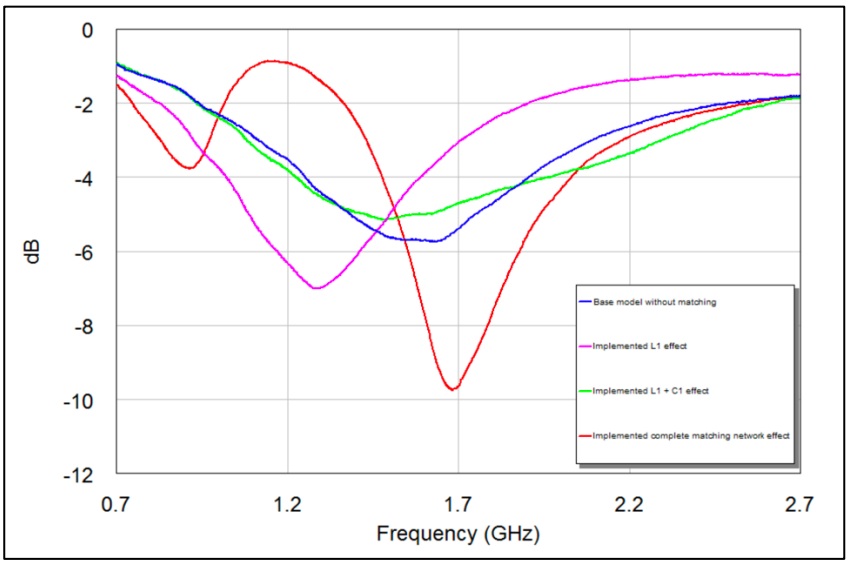

Figure 48: Evolution of the return losses after implementing and manually tuning every component

Finally, a comparison between the optimized matching network resulting return losses and the ones obtained after implementing and manually tuning it is carried out (Figure 49). It can be seen how, after adding all the components, the sum of every component's introduced error

makes the final model not able to reach the design goals and, so, not viable for its commercialization.

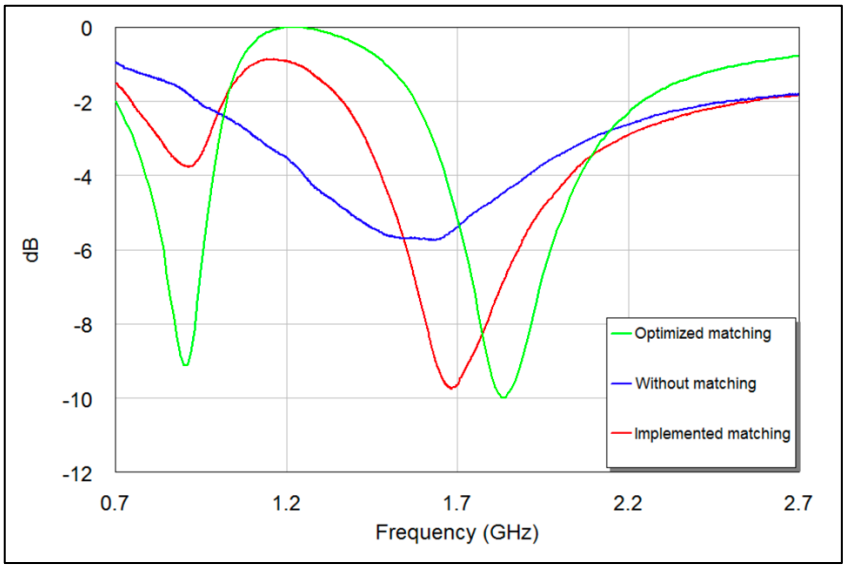

Figure 49: Comparison between the obtained return losses in the optimized and the implemented cases

4.5.3 Separation from the phantom hand

After not getting a viable candidate with the first studied design, it is necessary to find a new candidate. There are two main ways of doing so: starting from the beginning looking for a new architecture for the antenna or modifying the actual candidate in a way that makes it work properly in order to fit this project's goal.

As the first option can be taken at any time, the decision has been to try to modify somehow the actual candidate. Taking a look back to the reviewed literature, there is a fact that has a lot of influence in the antenna's behaviour that has not been considered, and this is the effect of the phantom hand. As explained in 2.2.6, the separation between the antenna and the human forearm can have a very large effect on the antenna's behaviour.

Therefore, and before starting all over with the design of a new prototype, the previous candidate has been modified by adding a 5mm thick methacrylate separation (Figure 50), so the space between the antenna and the is incremented to a total of 6mm (1 from the own FR4 surface and 5 from the added methacrylate).

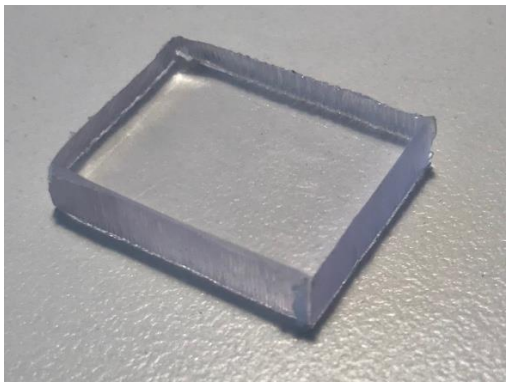

Figure 50: Piece of 5mm thick methacrylate used to separate the antenna from the phantom hand

The reason of using methacrylate is the lack of conductivity that is has, making it be almost invisible for the antenna. The methacrylate separator has been attached to the back of the ground plane ().

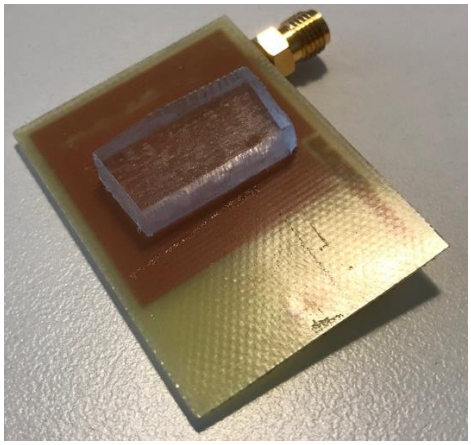

Figure 51: Addition of the methacrylate separator in the back of the antenna's ground plane

Once this last element is added, the new candidate (Figure 52) has been analysed with the same matching network as in the previous case, in order to see the direct effect of that introduced separation.

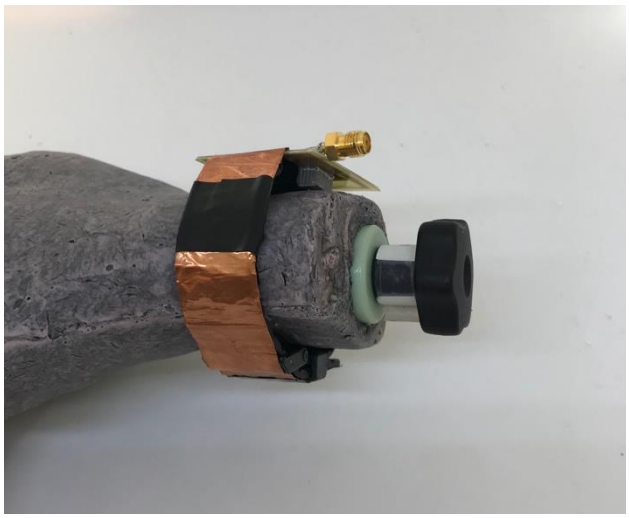

Figure 52: Final version of the new candidate, with the addition of the phantom hand and the 90mm enlargement

After exporting the analysed return losses for this renewed design, the resulting adaptation has suffered a great improvement in comparison with the previous case (Figure 53). This improvement makes the current prototype valid, having it a total bandwidth of 111MHz (846MHz to 957MHz) at the GSM band and 300MHz (1590MHz to 1890MHz) at the High Frequency band.

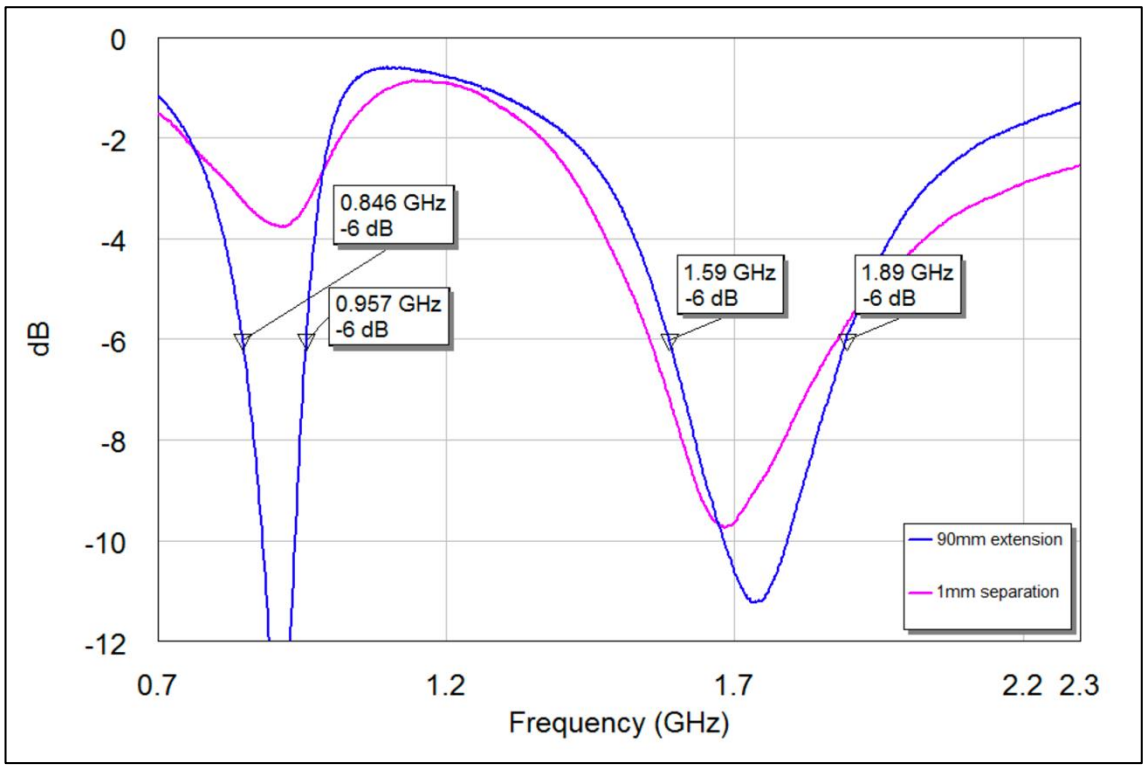

Figure 53: Measured S_{11} for the 1mm and 6mm separated cases

4.5.4 Not extended model

Once the candidate has been validated, a last test has been carried out: the extension of the ground plane has been eliminated in order to see its real effect on the antenna.

Results confirm the need of the 90mm extension, showing a really poor performance for this not extended model. Therefore, the initial simulations concluded fine at indicating the need of a larger ground plane for the antenna to be able to match the design goals.

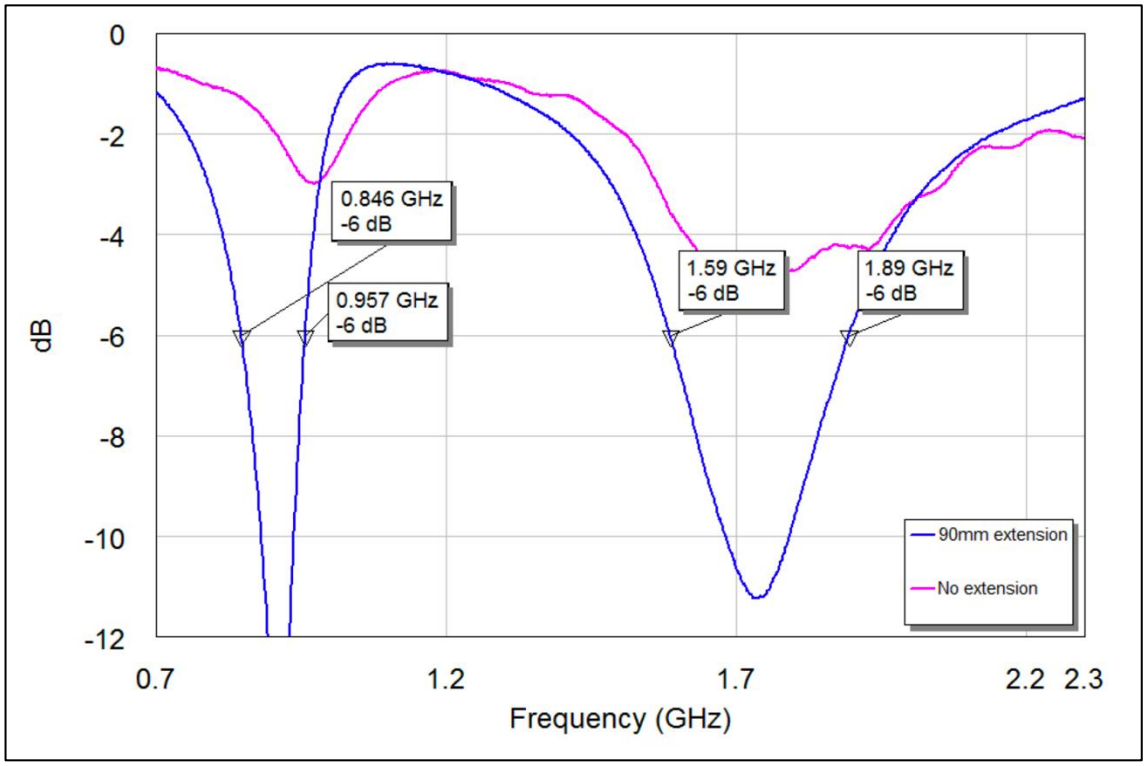

Figure 54: Return losses for the 90mm extended model and the not extended model

After all this testing, the resulting candidate is the 30 x 30 mm^2 ground plane, with a 90mm cooper tape extension and an extra separation of 5mm using 1mm thick methacrylate.

Nevertheless, radiation and antenna efficiencies have to be computed in order to see the real performance of the prototype.

4.5.5 Efficiency computation

Finally, the last study that the antenna has to pass is the radiation and the antenna efficiency.

The efficiency of an antenna is a ratio of the power delivered to the antenna in relation to the power that this antenna is capable of radiating. The higher the efficiency, the less power the antenna will need to radiate the same amount of power. A low efficiency antenna has most of the power absorbed as losses or reflected due to a bad impedance matching.

In order to compute the antenna efficiency, a SATIMO is used. This is composed by an anechoic chamber in which centre the antenna is placed. Then, through an own computer software, the simulation is configured, and the antenna efficiency of the antenna is detected through multiple sensors placed in an arch around the antenna (Figure 55).

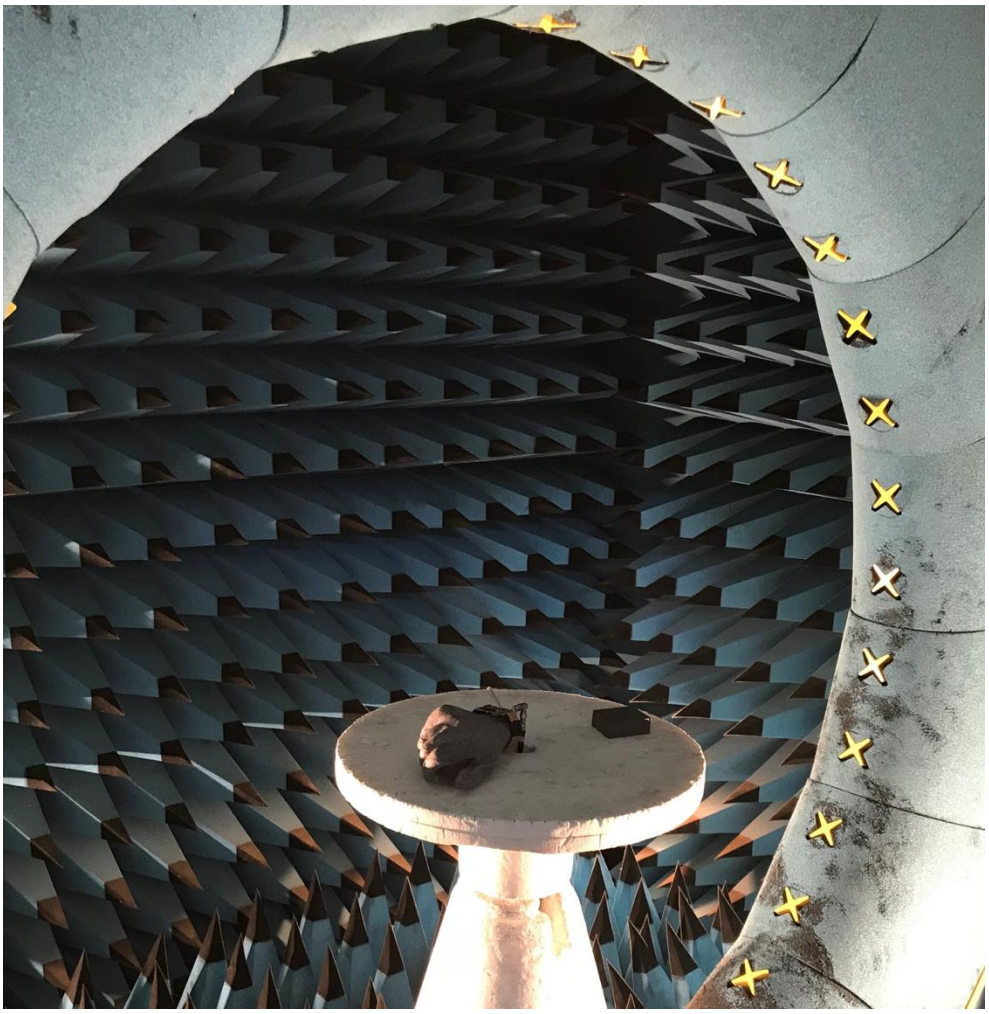

Figure 55: Prototype placed at the feeding platform of the SATIMO

In order to obtain an objective analysis from the efficiency results, the efficiency of three models will be computed:

- The actual candidate: 90mm extension and 6mm separation from the phantom hand.
- The base model: 90mm extension and 1mm separation from the phantom hand.

- Not enlarged model: Just to see the enlargement effects, a simulation without the 90mm cooper tape has been carried out.

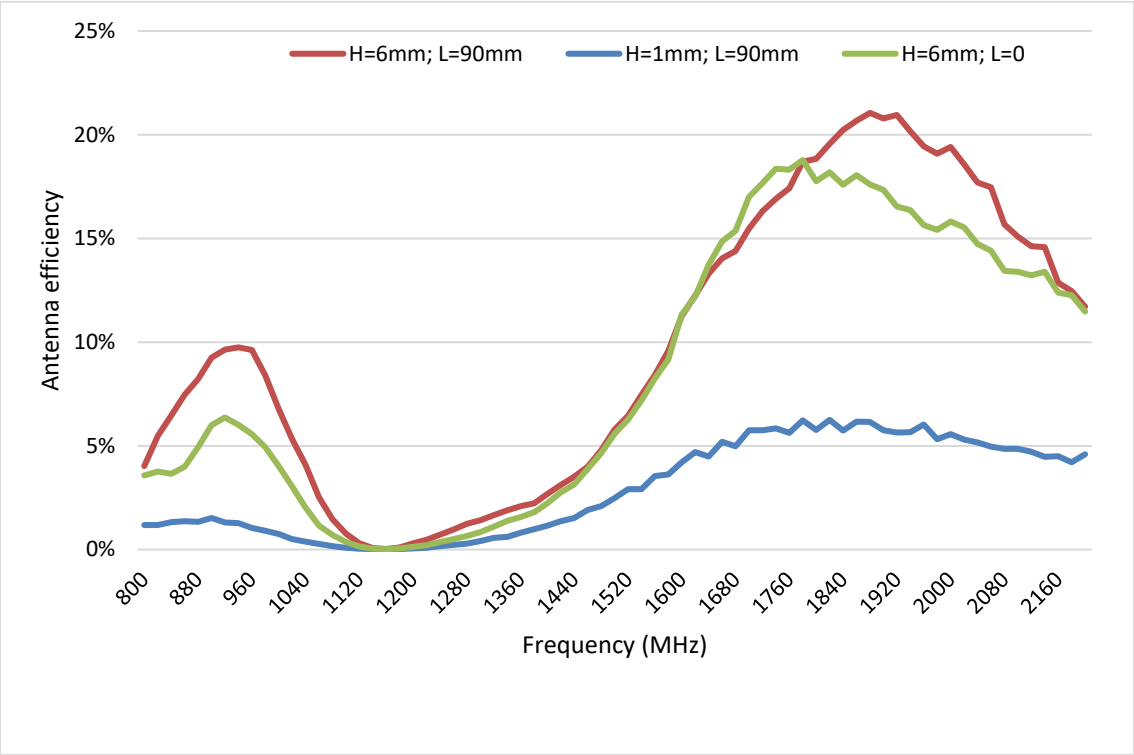

Figure 56: Antenna efficiencies for different antenna models

Results show (Figure 56) that the proposed candidate is actually the best one in terms of antenna efficiency, reaching a 10% in the GSM band and over a 20% in the High Frequency band.

It is also seen how the separation between the antenna and the phantom hand must be considered as a key factor in the design process of smartwatch application antennas. Proof of it is that in the 1mm separation model the antenna efficiency is drastically lower than in the 6mm separated models, not even reaching a 2,5% at the lower band (Table 7).

Table 7: Antenna efficiencies for the different models at the interest frequential regions

Model	824MHz	960MHz	MAX	1710MHz	1990MHz	MAX
H=6mm, L=90mm	5.5%	9.6%	9.8%	15.8%	19.2%	21%
H=1mm, L=90mm	1.2%	1%	1.5%	5.7%	5.4%	6.2%
H=6mm, L=0mm	3.7%	5.5%	6.3%	17.3%	15.6%	18.7%

Since the antenna efficiency is actually a version of the radiation efficiency made worse by the return losses (Equation 2), all three models' radiation efficiency has been computed. This parameter can be a good metric for the model's evaluation, since it shows how good an antenna can perform if it is properly adapted.

Equation 2: Radiation and antenna efficiencies relation formula

$$\eta_A = \eta_R \cdot (1 - |S_{11}|^2)$$

Starting with the discarded models, the radiation efficiency for the 1mm separated model is computed (Figure 57). In this case, the short distance between the antenna and the phantom hand makes the model unable to reach the design goals, even if it was perfectly adapted ($|S_{11}|$=0).

As long as the radiation efficiency is not at any point better by more of a 2% in comparison with the antenna efficiency, the chosen matching network can be considered the adequate for this model.

This result becomes the final evidence for the already explained effect of the phantom hand on the antenna's performance.

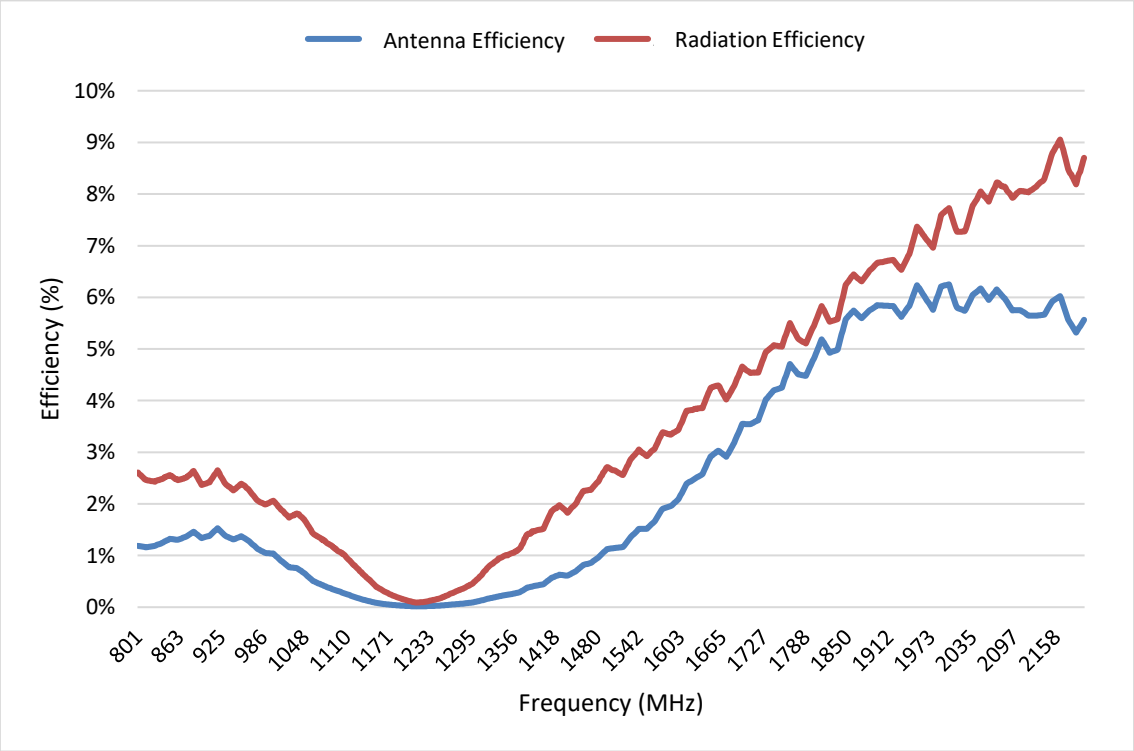

Figure 57: Comparison between the antenna and the radiation efficiencies for the 1mm separation and 90mm extension model

The second computed radiation efficiency is the not extended model's one (Figure 58). This prototype has a 6mm separation between the antenna and the phantom hand, and so it is expected to have a much higher efficiency than the 1mm separated model.

In this case, the introduction of the methacrylate separation plays a key role, not only improving the antenna efficiency but also making the antenna capable of reaching high enough efficiencies to be considered as a valid model if the matching network is improved.

Taking into account that this model has not passed through an individual adaptation process, and that it is the result of removing the extension from the main candidate, the resulting radiation efficiency opens a door to future investigation of the viability of a not extended model.

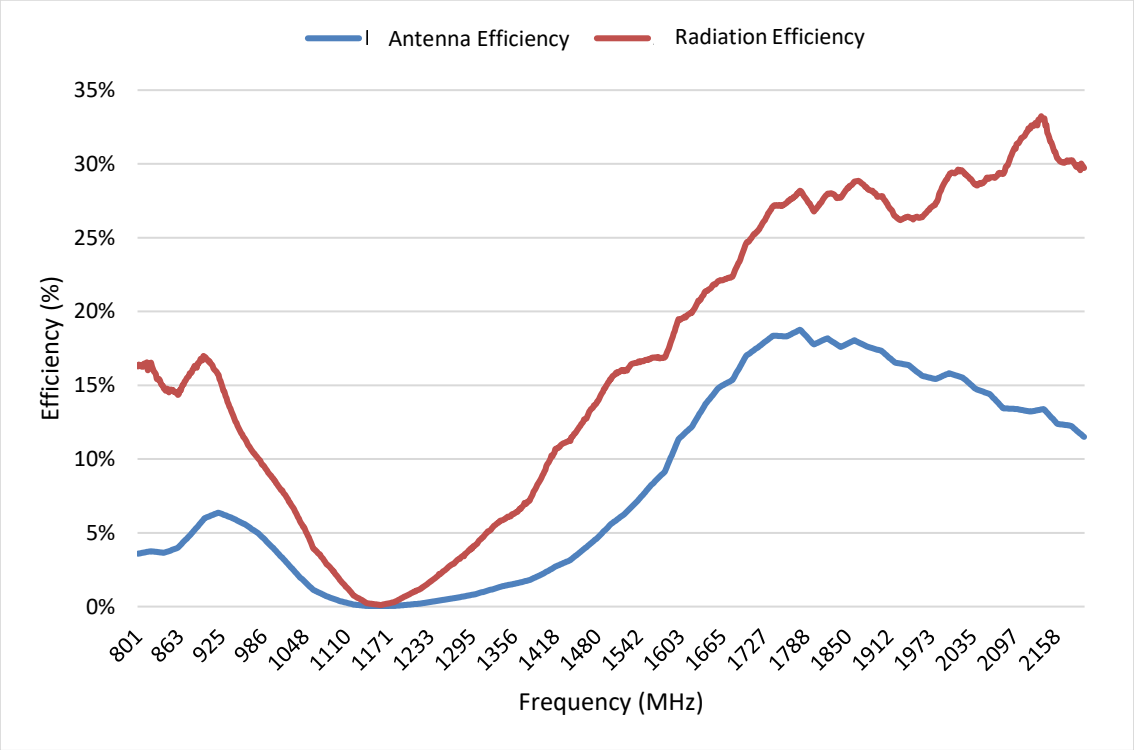

Figure 58: Comparison between the antenna and the radiation efficiencies for the 6mm separation and no-extension model

Lastly, the radiation efficiency for the main candidate is computed and compared to its antenna efficiency (Figure 59).

Although this model was expected to show a really high radiation efficiency values, due to the presence of not only the separation from the phantom hand but also the 90mm extension of the ground plane, the obtained results don't accomplish those expectations. It can be seen that at the interest bandwidths centre, there is almost no difference between the radiation and the antenna efficiencies. This means a) that the matching network is working properly at these frequencies and b) that the prototype has not a big improving margin.

Summing up, this results indicate the need of thinking back this model from the very beginning in case of wanting to improve its performance.

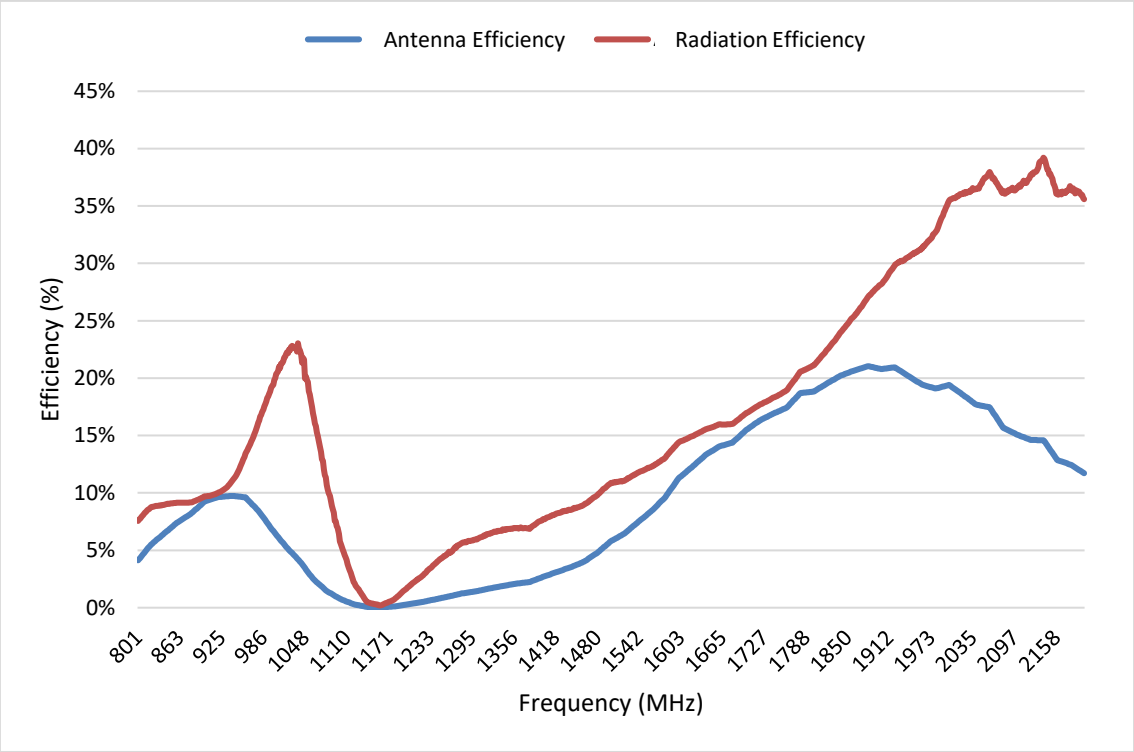

Figure 59: Comparison between the antenna and the radiation efficiencies for the main candidate, with a 6mm separation and a 90mm extension

5 Conclusions

5.1 Introduction

In this project, an antenna for smartwatch applications has been researched. The reviewed art in the second chapter has defined both the market needs and how the antenna must be characterised in order to fit actual smartwatches models. This way, a design and simulation process has been carried out in order to obtain a solid candidate to be implemented and tested.

In the fourth chapter of this work, three different prototypes have been implemented and tested. After analysing the obtained results from the three candidates, one of them has been chosen as a viable one. At the very end of the study, the resulting antenna efficiencies of the best candidate have shown that, although its performance could be considered as good enough for fitting the actual market, this design has a very small improvement margin.

5.2 Conclusions

The main goal for this project was to find an antenna for smartwatch applications capable of working at cell phone bands. After several months of investigation, design and implementation, the main goal has been reached and a working prototype has been proposed (Figure 60).

Furthermore, the following general conclusions for matters of smartwatch antenna's designing can be withdrawn:

- Dimensions: Starting with the reduced available space for the design, the Fractus Antenna's Antenna booster come out as a very good option for this kind of antennas. The fact of it making the rest of the ground plane actuate as a radiating surface allows the design to be more compact and low-profile.

  The option of enlarging the ground plane using a cooper tape has also been studied. At the design and simulation stage, this enlargement has shown a valuable improvement in comparison to the not extended models.

- Human body effect: This parameter has shown a huge effect on the antenna's behaviour. After carrying out different studies with different separations between the antenna and the phantom hand, it can be ensured that it is primordial to make that separation as longer as possible.

- Methodology: A project like this one would have never been possible if a severe methodology was followed. Therefore, the importance of defining the research steps and the path to follow even before starting with the state-of-the-art review has been proven to be a clue factor.

Additionally, it can be concluded that this project's limitations and the further research lines are:

- Limitations: The resulting prototypes have not been tested introducing the rest of a smartwatch elements, such as the framebox and the screen. As long as these elements may introduce changes in the antenna's performance, the actual results for the antenna once introduced on a real model cannot be ensured to be the same as the obtained.
- Further research lines: From this project's final point, many possible paths can be followed. Looking at the results, one of the most interesting investigation lines could be the study of a not extended model with a larger separation between the antenna and the phantom hand. This research could lead to a cheaper, easier to implement and better performing smartwatch antenna.

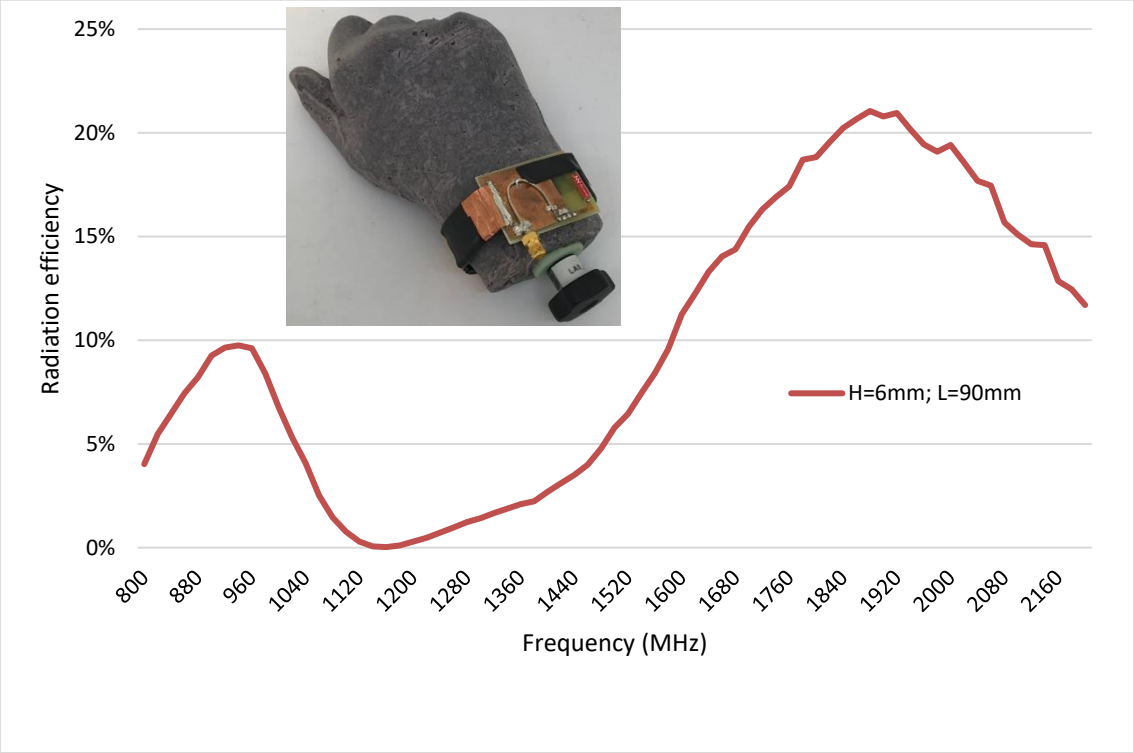

Figure 60: Image and radiation efficiency for the resulting working prototype

6 References

[1] https://www.forbes.com/global2000/#4958cf96335d

[2] Oscar Szymanczyk, “Historia de las telecomnunicaciones mundiales”. Dunken, 2013.

[3] Ira Sager, “Before IPhone and Android came Simon, the First Smartphones”. Bloomberg Businessweek. Bloomberg L.P. June 2012.

[4] Jeremy Rocher, “Sony Ericsson Bluetooth Watch MBW 100”. CNET, 2017.

[5] Saou-Wen Su, Cheng-Tse Lee, “Metal-Frame GPS Antenna for Smartwatch Applications”. Progress In Electromagnetics Research Letters, Vol. 62, 41-47, 2016.

[6] K. Zhao, Z. Ying, S. He. “Antenna Designs of Smart Watch for Cellular Communications by using Metal Belt”. 2015 9th European Conference on Antennas and Propagation (EuCAP), Lisbon, 2015, pp. 1-5.

[7] Y. Chen, T. Ku, “A Low-Profile Wearable Antenna Using a Miniature High Impedance Surface for Smartwatch Applications”. IEEE ANTENNAS AND WIRELESS PROPAGATION LETTERS, VOL. 15, 2016.

[8] W. Chen, C. Yang, W. Sin, “MIMO Antenna with Wi-Fi and Blue-Tooth for Smart Watch Applications”. 2015 IEEE MTT-S 2015 International Microwave Workshop Series on RF and Wireless Technologies for Biomedical and Healthcare Applications (IMWS-BIO), Taipei, 2015, pp. 212-213.

[9] D. Wu, S. Cheung, Q. Li, T. Yuk. “Slot Antenna for All-Metal Smartwatch Applications”. 2016 10th European Conference on Antennas and Propagation (EuCAP), Davos, 2016, pp. 1-4.

[10] C. Wu, K. Wong, Y. Lin, “Conformal Bluetooth Antenna for the Watch-Type Wireless Communication Device Application”. 2007 IEEE Antennas and Propagation Society International Symposium, Honolulu, HI, 2007, pp. 4156-4159.

[11] T. Ku, Y. Chen. “Wearable Antenna Design on Finite-Size High Impedance Surfaces for Smart-Watch Applications”. 2015 IEEE International Symposium on Antennas and Propagation & USNC/URSI National Radio Science Meeting, Vancouver, BC, 2015, pp. 938-939.

[12] J. Anguera, C. Picher, A. Andújar, and C. Puente, “Concentrated Antennaless Wireless Device Providing Operability in Multiple Frequency Regions”, patent. app. US 61/671,906

[13] A. Andújar and J. Anguera, “Scattered Virtual Antenna Technology for Wireless Devices”, patent app. US61/837265

[14] J. Anguera, A. Andújar, and C. Puente, “Wireless handheld devices, radiation systems and manufacturing methods”, patent app. US13/946922J. Anguera, N. Toporcer, and A. Andújar, “Slim bar booster for electronics devices”, patent app. EP14178369

[15] J. Anguera, A. Andújar, C. Puente, and J. Mumbrú, “AntennaLess Wireless Device”, patent app. WO 2010/015365

[16] J. Anguera, A. Andújar, C. Puente, and J. Mumbrú, “AntennaLess Wireless Device Capable of Operation in Multiple Frequency Regions”, patent app. WO 2010/015364

[17] J. Anguera, C. Borja, C. Picher, and A. Andújar, “Wireless Device Providing Operability for Broadcasting Standards and Method Enabling such Operability”, patent app. WO/2010/145825

[18] J. Anguera and A. Andújar, “AntennaLess Wireless Device Comprising One or More Bodies”, patent app. WO 2011/095330

[19] A. Andújar, J. Anguera, C. Puente, and C. Picher, “Wireless Device Capable of Multiband MIMO Operation”, patent app. WO 2012/017013

[20] J. Anguera, A. Andújar, C. Puente, J. Mumbrú, “Antennaless wireless device capable of operation in multiple frequency regions”, US Patent 8,237,615, 2012

[21] J. Anguera, A. Andújar, C. Puente, J. Mumbrú, “Antennaless wireless”, US Patent 8,203,492, 2012

[22] A. Andújar, J. Anguera, and C. Puente, “Antenna boosters as a Compact Antenna Technology for Wireless Handheld Devices”, IEEE Transactions on Antennas and Propagation, vol.59, nº5, pp.1668-1677, May.2011.

[23] A. Andújar, J. Anguera, C. Picher, and C. Puente, “Human Head Interaction Over Antenna booster Antenna Technology: Functional and Biological Analysis”, Progress In Electromagnetics Research, B Vol. 41, pp-153-185, 2012.

[24] A. Andújar and J. Anguera, “On the Radiofrequency System of Antenna booster Antenna Technology”, Electronics Letters, vol.48, nº14, pp. 815-817, July 2012

[25] J. Anguera and A. Andújar, “Ground Plane Contribution in Wireless Handheld Devices using Radar Cross Section Analysis”, Progress In Electromagnetics Research M, vol.26, pp-101-114, 2012

[26] A. Andújar and J. Anguera, “Multiband Coplanar Antenna booster Antenna Technology”, Electronics Letters, vol.48, nº21, pp. 1326-1328, Oct. 2012

[27] A. Andújar and J. Anguera, “Magnetic Boosters for Multi-band Operation”, Microwave and Optical Technology Letters, vol.55, nº1, pp.65-75, January 2013

[28] Jaume Anguera, Aurora Andújar, Minh-Chau Huynh, Charlie Orlenius, Cristina Picher, and Carles Puente, “Advances in Antenna Technology for Wireless Handheld Devices”, International Journal on Antennas and Propagation, Volume 2013, Article ID 838364.

[29] Jaume Anguera, Aurora Andújar, and Carlos García, “Multiband and Small Coplanar Antenna System for Wireless Handheld Devices”, IEEE Transactions on Antennas and Propagation, vol.61, nº 7, pp. 3782-3789, July 2013.

[30] Aurora Andújar, Jaume Anguera, and Yolanda Cobo, “Distributed Systems Robust to Hand Loading based on Non-Resonant Elements”, Microwave and Optical Technology Letters, vol.55, nº10, pp.2307-2317, Oct. 2013.

[31] Aurora Andújar and Jaume Anguera, “MIMO Multiband Antenna System Combining Resonant and Non-Resonant Elements”, Microwave and Optical Technology Letters, vol.56, nº5, pp.1076-1084, May 2014.

[32] Cristina Picher, Jaume Anguera, Aurora Andújar, and Adrián Bujalance, “Non-resonant element in a slotted ground plane for multiband antenna operation”, ETRI Journal, vol.36, nº 5, pp. 835- 840, October, 2014.

[33] Cristina Picher, Jaume Anguera, Aurora Andújar, Carles Puente, and Adrián Bujalance, “Concentrated Antenna booster Antenna Technology for Multiband Operation in Handset Devices”, Radioengineering, Vol. 23, nº. 4, Dec. 2014. pp.1061-1070.

[34] José Luis Leiva, Aurora Andújar, Jaume Anguera, “On the behavior of a compact antenna system with non-resonant elements: human head analysis”, International Journal of Electronics, 2015, pp.1-20.

[35] Aurora Andújar and Jaume Anguera, “MIMO Multiband Antenna System with Non-Resonant Elements”, Microwave and Optical Technology Letters, vol.57, nº1, pp.183-190, Jan. 2015

[36] Cristina Picher, Jaume Anguera, Adrián Bujalance, Aurora Andújar, “Antenna booster Antenna Technology using a Self-Diplexed Matching Network for Multiband Operation”, Microwave and Optical Technology Letters, vol.58, nº2, pp.453-461, February 2016.

[37] J. Anguera and A. Andújar, “Antenna booster antenna technology for wearable devices”, patent app. US15/449,551

[38] Jaume Anguera, Cristina Picher, Adrián Bujalance, and Aurora Andújar, “Antenna booster Antenna Technology for Smartphones and Tablets”, Microwave and Optical Technology Letters, vol.58, nº6, pp.1289-1294, June 2016.

[39] Lluis Grau, “On the isolation of Antenna booster Antenna Technology in Wireless MIMO Devices”. La Salle URL, 2016.